Current-density implementation for calculating flexoelectric coefficients

Cyrus E. Dreyer, Massimiliano Stengel, and David Vanderbilt

Current-density implementation for calculating flexoelectric coefficients

Cyrus E. Dreyer,[1] Massimiliano Stengel,[2, 3] and David Vanderbilt[1]

[1]*Department of Physics and Astronomy, Rutgers University, Piscataway, New Jersey 08845-0849, USA*
[2]*ICREA-Institució Catalana de Recerca i Estudis Avançats, 08010 Barcelona, Spain*
[3]*Institut de Ciència de Materials de Barcelona (ICMAB-CSIC), Campus UAB, 08193 Bellaterra, Spain*
(Dated: August 1, 2018)

The flexoelectric effect refers to polarization induced in an insulator when a strain gradient is applied. We have developed a first-principles methodology based on density-functional perturbation theory to calculate the elements of the bulk clamped-ion flexoelectric tensor. In order to determine the transverse and shear components directly from a unit cell calculation, we calculate the current density induced by the adiabatic atomic displacements of a long-wavelength acoustic phonon. Previous implementations based on the charge-density response required supercells to capture these components. At the heart of our approach is the development of an expression for the current-density response to a generic long-wavelength phonon perturbation that is valid for the case of nonlocal pseudopotentials. We benchmark our methodology on simple systems of isolated noble gas atoms, and apply it to calculate the clamped-ion flexoelectric constants for a variety of technologically important cubic oxides.

I. INTRODUCTION

The flexoelectric (FxE) effect, where polarization is induced by a strain gradient, is universal in all insulators. As devices shrink to the micro and nano scale, large strain gradients can occur, and therefore the FxE effect can play a significant role in the properties of such devices, influencing the so-called dielectric dead layer,[1] domain walls and domain structure,[2–4] relative permittivity and Curie temperature,[5,6] critical thickness of films to exhibit switchable polarization,[7] and spontaneous polarization in the vicinity of twin and antiphase boundaries.[8] Also, the FxE effect can be exploited for novel device design paradigms, such as piezoelectric "meta-materials" constructed from nonpiezoelectric constituents,[9,10] or mechanical switching of ferroelectric polarization.[11,12]

One of the crucial limitations to understanding and exploiting the FxE effect is the lack of a clear experimental and theoretical consensus on the size and sign of the FxE coefficients, even in commonly studied materials such at $SrTiO_3$ and $BaTiO_3$.[13,14] A key element to forming this understanding is the development of an efficient first-principles methodology to calculate all of the components of the bulk FxE tensor. Recently, Stengel,[15] and Hong and Vanderbilt[16,17] (HV), developed the formalism for calculating the full bulk FxE tensor from first principles.[18]

Each element of the FxE tensor has a "clamped-ion" (CI) contribution, arising from the effect of the strain gradient on the valence electrons in the crystal, and a "lattice-mediated" (LM) contribution, arising from internal relaxations induced by the applied strain and strain gradient.[15,17] In Refs. 16 and 17, HV described an implementation for calculating the bulk CI and LM longitudinal FxE coefficients (i.e., the coefficients relating the induced polarization in direction α to a gradient of uniaxial strain $\varepsilon_{\alpha\alpha}$, also in direction α). Their methodology involved using density functional theory (DFT) to calculate the real-space response of the charge density to

atomic displacements in a simple $N \times 1 \times 1$ bulk supercell containing N repitions of the primitive bulk cell.

In Ref. 19, Stengel developed a strategy that allowed a calculation of the full FxE response for cubic $SrTiO_3$ based in part on the charge-density response to a long-wavelength acoustic phonon, and in part on large slab supercell calculations (repeated slabs separated by vacuum). The first part of this methodology allowed the LM contributions to all bulk FxE tensor elements, as well as the CI contributions to the longitudinal coefficients, to be determined from linear-response calculation on a single unit cell using density-functional perturbation theory (DFPT).[20] However, the "transverse" and "shear" CI contributions[17,19,21] had to be calculated indirectly by relating them to the open-circuit electric field appearing across the slab when a long wavelength acoustic phonon was applied to the slab supercell as a whole. As a result, this implementation required DFPT calculations to be performed on large slab supercells.

The implementation described in Ref. 19 thus provides a methodology for calculating the full FxE tensor for a given material. However, the reliance on computationally intensive slab supercell calculations for the transverse and shear CI coefficients represents a significant limitation to efficient calculation, especially in complex materials. Therefore, it is highly desirable to develop an approach that allows the full bulk FxE tensor, including its longitudinal, transverse, and shear components, to be obtained from DFPT calculations on single unit cells.

The essential problem is that single-unit-cell DFPT calculations that determine only the charge-density response to a long-wavelength phonon, as in Ref. 19, are incapable of revealing the transverse and shear CI contributions, since the induced charge is proportional to the *divergence* of the polarization, which is absent for transverse phonons. To go further, it is necessary to compute the induced *polarization itself*. Unfortunately, the well-known Berry-phase formulation[22,23] of the electric polarization is useless here, since it provides only the to-

tal polarization, which averages to zero over a phonon wavelength. Instead, we need access to the spatially resolved polarization on the scale of the wavelength. The only clear path to obtaining this local polarization is via its relation to the adiabatic current density.[15,17,24] Thus, the desired methodology is one that computes the spatially resolved *current density* induced by a strain gradient perturbation[15,17,24] in the context of long-wavelength longitudinal *and transverse* phonons.

The microscopic current density is, of course, just proportional to the quantum-mechanical probability current, as discussed in any standard textbook.[25] However, this standard formula assumes a local Hamiltonian of the form $H = p^2/2m + V$ with a local potential V. Thus, it becomes problematic if the Hamiltonian of interest contains *nonlocal* potentials, as the probability current no longer satisfies the continuity equation.[26] This issue is very relevant in the context of DFT, since most popular implementations make use of a plane-wave basis set with a pseudopotential approximation to reduce the size of the basis set by avoiding an explicit description of the core electrons. Virtually all modern pseudopotential implementations contain nonlocal potentials in the form of projectors that operate on the wavefunctions.[27–30] Therefore, the standard formula for the current density is not a fit starting point for the current-response theory that we have in mind (we expand on these considerations in Sec. III B).

The definition and calculation of the microscopic current density in a nonlocal pseudopotential context is a rather general problem that has received considerable previous attention[26,31–36] in view of its application to the calculation of magnetic susceptibility,[32–36] nuclear magnetic resonance chemical shifts,[37] electron paramagnetic resonance g tensors,[38] and so forth. Unfortunately a general, systematic solution that is appropriate to our scopes has not emerged yet. To see why this is challenging, it is important to note that the continuity equation is only one of the criteria that must be satisfied by a physically meaningful definition of the current density. Two other criteria are important. First, the formula must also reduce to the textbook expression in regions of space that lie outside the range of the nonlocal operators (pseudopotentials are typically confined to small spheres surrounding the atoms). Second, it must reduce to the well-known expressions for the macroscopic current in the long-wavelength limit. The approaches that have been proposed so far have either been specialized to a certain physical property (e.g., dielectric[31] or diamagnetic[34] response), or limited in scope to a subset of the above criteria. For example, Li *et al.*[26] proposed a strategy that guarantees charge continuity by construction but does not satisfy the two additional criteria, as we shall see in Sec. III B.

In addition to the technical challenges related to nonlocal pseudopotentials, there is another complication associated with the calculation of the flexoelectric coefficients using the current density in bulk. Namely, the bulk

nonlongitudinal responses contain a contribution coming from the gradients of the local rotations in the crystal. This "circulating rotation-gradient" (CRG) contribution, derived in Ref. 24 (where it is referred to as a "dynamic" or "gauge-field" term), must be treated carefully when comparing our calculations with previous results. We will discuss this point in Sec. III D.

In this work we develop a first-principles methodology based on DFT to calculate the full bulk CI FxE tensor from a single unit cell. At the heart of our technique lies the introduction of a physically sound microscopic current-density operator in the presence of nonlocal pseudopotentials that fulfills all criteria that we stated in the above paragraphs: (i) it satisfies the continuity equation; (ii) the contribution of the nonlocal pseudopotentials is correctly confined to the atomic spheres; and (iii) it reduces to the macroscopic velocity operator in the long-wavelength limit. We will discuss our approach for calculating the current density in the context of earlier works, and how it applies to the problem of calculating bulk FxE coefficients. Finally, we will demonstrate that the results for the CI FxE coefficients from our current-density implementation are in excellent agreement with the previous charge-density-based DFT implementations described above,[17,19] confirming that it is an accurate and efficient method for calculating the FxE response of materials.

The paper is organized as follows. In Sec. II we outline the general approach to determining FxE coefficients; in Sec. III we give the formalism used in our calculations of the current density; in Sec. IV we provide details of the implementation of the formalism; Sec. V presents benchmark tests for the simple case of isolated noble gas atoms, and results for several technologically important, cubic oxide compounds; in Sec. VI, we discuss some technical issues that are associated with the current density in the presence of nonlocal pseudopotentials; we conclude the paper in Sec. VII.

II. APPROACH

The goal of this work is to calculate the bulk CI flexoelectric tensor elements

$$\mu^{I}_{\alpha\beta,\omega\nu} = \frac{dP_\alpha}{d\eta_{\beta,\omega\nu}}, \tag{1}$$

where P_α is the polarization in direction α, and

$$\eta_{\beta,\omega\nu} = \frac{\partial^2 u_\beta}{\partial r_\omega \partial r_\nu} \tag{2}$$

is the strain gradient tensor, where u_β is the β component of the displacement field. The superscript "I" indicates that the tensor elements are defined with respect to the unsymmetrized displacements;[39] superscripts "II" will be used to indicate tensor elements defined with respect to symmetrized strain.

Calculating the polarization in Eq. (1) is tricky from a quantum-mechanical standpoint, as it does not correspond to the expectation value of a well-defined operator. As mentioned above, the Berry-phase method[22,23] can be used to obtain the formal macroscopic polarization averaged over the cell. However, we require access to the local polarization *density* $P_\alpha(\mathbf{r})$. Although the static microscopic polarization density is not well defined in a quantum mechanical context, at the linear-response level the *induced* polarization $P_{\alpha,\lambda}(\mathbf{r}) = \partial P_\alpha(\mathbf{r})/\partial\lambda$ resulting from a small change in parameter λ can be equated to the local current flow via $\partial P_\alpha(\mathbf{r})/\partial\lambda = \partial J_\alpha(\mathbf{r})/\partial\dot{\lambda}$, where $\dot{\lambda}$ is the rate of change of the adiabatic parameter, λ. Following the approach of Ref. 15, we now consider an adiabatic displacement of sublattice κ (i.e., a given atom in the unit cell along with all of its periodic images) of a crystal in direction β as given by

$$u_{\kappa\beta}(l,t) = \lambda_{\kappa\beta\mathbf{q}}(t)e^{i\mathbf{q}\cdot\mathbf{R}_{l\kappa}} \tag{3}$$

where l is the cell index. In this case the induced local polarization density $P_{\alpha,\kappa\beta\mathbf{q}}(\mathbf{r})$ in direction α induced by mode $\kappa\beta$ of wavevector $\mathbf{q}$ is

$$P_{\alpha,\kappa\beta\mathbf{q}}(\mathbf{r}) = \frac{\partial J_\alpha(\mathbf{r})}{\partial\dot{\lambda}_{\kappa\beta\mathbf{q}}}. \tag{4}$$

Using the fact that the linearly induced current will be modulated by a phase with the same wavevector as the perturbation in Eq. (3), we can define

$$P^{\mathbf{q}}_{\alpha,\kappa\beta}(\mathbf{r}) = P_{\alpha,\kappa\beta\mathbf{q}}(\mathbf{r})e^{-i\mathbf{q}\cdot\mathbf{r}}, \tag{5}$$

which is therefore a lattice-periodic function. This quantity, the *cell-periodic part of the first-order induced polarization density*, will play a central role in our considerations. It is also convenient to define

$$\overline{P}^{\mathbf{q}}_{\alpha,\kappa\beta} \equiv \frac{1}{\Omega}\int_{\text{cell}} P^{\mathbf{q}}_{\alpha,\kappa\beta}(\mathbf{r})d^3r, \tag{6}$$

where Ω is the cell volume, as the cell average of this response. In Ref. 15 it was shown that the CI flexoelectric tensor elements are given by the second wavevector derivatives of $\overline{P}^{\mathbf{q}}_{\alpha,\kappa\beta}$ via

$$\mu^{\text{I}}_{\alpha\beta,\omega\nu} = -\frac{1}{2}\sum_\kappa \frac{\partial^2 \overline{P}^{\mathbf{q}}_{\alpha,\kappa\beta}}{\partial q_\omega \partial q_\nu}\bigg|_{\mathbf{q}=0}. \tag{7}$$

This formulation suggests that it may be possible to compute the polarization responses $\overline{P}^{\mathbf{q}}_{\alpha,\kappa\beta}$ entirely from a single-unit-cell calculation, similar to the way that phonon responses are computed in DFPT. In fact, this is the case. The formalism necessary to compute these responses at the DFT level will be presented in the next sections, giving access to an efficient and robust means to compute the flexoelectric coefficients through Eq. (7).

III. FORMALISM

Given a time-dependent Hamiltonian with a single-particle solution $\Psi(t)$, the current density at a point $\mathbf{r}$ in Cartesian direction α can be written

$$J_\alpha(\mathbf{r}) = \langle\Psi(t)|\hat{\mathcal{J}}_\alpha(\mathbf{r})|\Psi(t)\rangle \tag{8}$$

where $\hat{\mathcal{J}}_\alpha(\mathbf{r})$ is the current-density operator (a caret symbol over a quantity will indicate an operator). We will first address how to treat the time-dependent wavefunctions (Sec. III A), and then discuss the form of the current-density operator in (Sec. III B) .

A. Adiabatic density-functional perturbation theory

1. Adiabatic response

We write the time-dependent Schrödinger equation as

$$i\frac{\partial}{\partial t}|\Psi\rangle = \hat{H}(\lambda(t))|\Psi\rangle. \tag{9}$$

where $\hat{H}(\lambda(t))$ is the Hamiltonian, and λ parametrizes the time-dependent atomic motion. Since we are interested in the current density resulting from adiabatic displacements, we expand the wavefunction $|\Psi(t)\rangle$ to first order in the velocity, $\dot{\lambda}$:[40–42]

$$|\Psi(t)\rangle \simeq e^{i\gamma(t)}e^{i\phi(\lambda(t))}[|\psi(\lambda(t))\rangle + \dot{\lambda}(t)|\delta\psi(\lambda(t))\rangle], \tag{10}$$

where $|\psi(\lambda)\rangle$ is the lowest-energy eigenfunction of the time-independent Hamiltonian at a given λ, and $|\delta\psi(\lambda)\rangle$ is the first order adiabatic wavefunction [defined by Eq. (10)]; $\gamma(t) = -\int_0^t E(\lambda(t'))dt'$ is the dynamic phase, with $E(\lambda)$ being the eigenenergy of $|\psi(\lambda)\rangle$; $\phi(\lambda(t)) = \int_0^t \langle\psi(\lambda(t'))|i\partial_t\psi(\lambda(t'))\rangle dt'$ is the geometric Berry phase[43] (we have used the shorthand $\partial_t = \partial/\partial t$). We work in the parallel-transport gauge, $\langle\psi(\lambda)|i\partial_\lambda\psi(\lambda)\rangle = 0$, so the Berry phase contribution vanishes.

Equation (10) is written assuming a single occupied band, but in the multiband case we shall let the evolution be guided by multiband parallel transport instead. In this case, the first-order wavefunctions, $\delta\psi_n$, given by adiabatic perturbation theory,[40–42] are

$$|\delta\psi_n\rangle = -i\sum_m^{\text{unocc}}|\psi_m\rangle\frac{\langle\psi_m|\partial_\lambda\psi_n\rangle}{\epsilon_n - \epsilon_m}, \tag{11}$$

where ϵ_n is the eigenvalue of the nth single particle wavefunction, and ∂_λ is shorthand for $\partial/\partial\lambda$. The wavefunction $|\partial_\lambda\psi_n\rangle$ is the first-order wavefunction resulting from the *static* perturbation

$$|\partial_\lambda\psi_n\rangle = \sum_m^{\text{unocc}}|\psi_m\rangle\frac{\langle\psi_m|\partial_\lambda\hat{H}|\psi_n\rangle}{\epsilon_n - \epsilon_m}, \tag{12}$$

which is the quantity calculated in conventional DFPT implementations.[20,44]

2. Density functional theory

We will implement the calculations of the current density in the context of plane-wave pseudopotential DFT, so the single-particle wavefunctions we will use in Eq. (11) are solutions to the Kohn-Sham equation for a given band n and wavevector $\mathbf{k}$,

$$\hat{H}_{\mathrm{KS}}|\psi_{n\mathbf{k}}\rangle = \epsilon_{n\mathbf{k}}|\psi_{n\mathbf{k}}\rangle. \tag{13}$$

where the Kohn-Sham Hamiltonian is

$$\hat{H}_{\mathrm{KS}} = \hat{T}_{\mathrm{s}} + \hat{V}_{\mathrm{H}} + \hat{V}_{\mathrm{XC}} + \hat{V}_{\mathrm{ext}}^{\mathrm{loc}} + \hat{V}_{\mathrm{ext}}^{\mathrm{nl}}. \tag{14}$$

Here $\hat{T}_{\mathrm{s}}$ is the single-particle kinetic energy, $\hat{V}_{\mathrm{H}}$ is the Hartree potential, $\hat{V}_{\mathrm{XC}}$ is the exchange correlation potential, and the external potential contains both a local and nonlocal part (last two terms). We will consider norm-conserving, separable, Kleinmann-Bylander type[29] pseudopotentials. The form of the nonlocal potential (henceforth referred to as $\hat{V}^{\mathrm{nl}}$) is given by Eq. (C2). We will drop the "KS" subscript from here on. Note that, although we focus on norm-conserving pseudopotentials in this work, the issues pertaining to nonlocal potentials that will be discussed in Sec. III B would apply to ultrasoft[27] and projector augmented wave (PAW)[30] potentials as well.

3. Polarization response

Using the expansion in Eq. (10), the first-order one-particle density matrix is

$$\delta\hat{\rho} = \dot{\lambda}\frac{2}{N_k}\sum_{n\mathbf{k}}\left(|\delta\psi_{n\mathbf{k}}\rangle\langle\psi_{n\mathbf{k}}| + |\psi_{n\mathbf{k}}\rangle\langle\delta\psi_{n\mathbf{k}}|\right) \tag{15}$$

where the factors $(2/N_k)\sum_{n\mathbf{k}}$ take care of the spin degeneracy, sum over occupied Bloch bands, and average over the Brillouin zone. A monochromatic perturbation such as that of Eq. (3) always comes together with its Hermitian conjugate, coupling states at $\mathbf{k}$ with those at $\mathbf{k} \pm \mathbf{q}$, so that each perturbed wavefunction has two components that we refer as $\delta\psi_{n,\mathbf{k}+\mathbf{q}}$ and $\delta\psi_{n,\mathbf{k}-\mathbf{q}}$ respectively. We wish to select the cross-gap response at $+\mathbf{q}$, so we project onto this component of the density matrix to obtain[45]

$$\delta\hat{\rho}_{\mathbf{q}} = \dot{\lambda}\frac{2}{N_k}\sum_{n\mathbf{k}}\left(|\delta\psi_{n,\mathbf{k}+\mathbf{q}}\rangle\langle\psi_{n\mathbf{k}}| + |\psi_{n\mathbf{k}}\rangle\langle\delta\psi_{n,\mathbf{k}-\mathbf{q}}|\right). \tag{16}$$

Specializing now to the perturbation of Eq. (3), the corresponding polarization response is

$$P_{\alpha,\kappa\beta\mathbf{q}}(\mathbf{r}) = \frac{2}{N_k}\sum_{n\mathbf{k}}\left[\langle\psi_{n\mathbf{k}}|\hat{\mathcal{J}}_\alpha(\mathbf{r})|\delta\psi_{n\mathbf{k},\mathbf{q}}^{\kappa\beta}\rangle \right.$$
$$\left. + \langle\delta\psi_{n\mathbf{k},-\mathbf{q}}^{\kappa\beta}|\hat{\mathcal{J}}_\alpha(\mathbf{r})|\psi_{n\mathbf{k}}\rangle\right]. \tag{17}$$

Using Eqs. (11) and (12), the needed first-order wave functions are

$$|\delta\psi_{n\mathbf{k},\mathbf{q}}^{\kappa\beta}\rangle = -i\sum_m^{\mathrm{unocc}}|\psi_{m\mathbf{k}+\mathbf{q}}\rangle\frac{\langle\psi_{m\mathbf{k}+\mathbf{q}}|\partial_{\lambda_{\kappa\beta\mathbf{q}}}\hat{H}|\psi_{n\mathbf{k}}\rangle}{(\epsilon_{m\mathbf{k}+\mathbf{q}} - \epsilon_{n\mathbf{k}})^2}. \tag{18}$$

For Eq. (7), we require the cell-average of the $\mathbf{q}$-dependent polarization response [Eq. (6)]. Defining the operator

$$\hat{\mathcal{J}}_\alpha(\mathbf{q}) = \frac{1}{\Omega}\int_{\mathrm{cell}}d^3r\, e^{-i\mathbf{q}\cdot\mathbf{r}}\,\hat{\mathcal{J}}_\alpha(\mathbf{r}), \tag{19}$$

Eq. (6) can be written

$$\overline{P}_{\alpha,\kappa\beta}^{\mathbf{q}} = \frac{2}{N_k}\sum_{n\mathbf{k}}\left[\langle\psi_{n\mathbf{k}}|\hat{\mathcal{J}}_\alpha(\mathbf{q})|\delta\psi_{n\mathbf{k},\mathbf{q}}^{\kappa\beta}\rangle \right.$$
$$\left. + \langle\delta\psi_{n\mathbf{k},-\mathbf{q}}^{\kappa\beta}|\hat{\mathcal{J}}_\alpha(\mathbf{q})|\psi_{n\mathbf{k}}\rangle\right]. \tag{20}$$

The ground-state and first-order wavefunctions can be expressed in terms of cell-periodic Bloch functions in the normal way

$$\langle\mathbf{s}|\psi_{n\mathbf{k}}\rangle = u_{n\mathbf{k}}(\mathbf{s})e^{i\mathbf{k}\cdot\mathbf{s}}, \quad \langle\mathbf{s}|\delta\psi_{n\mathbf{k},\mathbf{q}}^{\kappa\beta}\rangle = \delta u_{n\mathbf{k},\mathbf{q}}^{\kappa\beta}(\mathbf{s})e^{i(\mathbf{k}+\mathbf{q})\cdot\mathbf{s}} \tag{21}$$

(Indices $\mathbf{s}$ and $\mathbf{s}'$ are not to be confused with the point $\mathbf{r}$ at which the current density is evaluated.) Using this notation, the cell-periodic first-order static wavefunction is written $|\partial_\lambda u_{n\mathbf{k},\mathbf{q}}^{\kappa\beta}\rangle$, which is equivalent to $|u_{n\mathbf{k},\mathbf{q}}^{\tau_{\kappa\beta}}\rangle$ in the notation of Gonze and Lee[44] and $|\Delta u_n^{\mathbf{k}+\mathbf{q}}\rangle$ in the notation of Baroni et al.[20]

By factoring out the phases with wavevector $\mathbf{k}$ and $\mathbf{q}$, we can insure that we only consider cell-periodic quantities, and therefore all calculations can be performed on a unit cell.[20] To this end, we define a cell-periodic operator[46]

$$\hat{\mathcal{J}}_\alpha^{\mathbf{k},\mathbf{q}} = e^{-i\mathbf{k}\cdot\hat{\mathbf{r}}}\hat{\mathcal{J}}_\alpha(\mathbf{q})e^{i(\mathbf{k}+\mathbf{q})\cdot\hat{\mathbf{r}}}. \tag{22}$$

Using the fact that $\hat{\mathcal{J}}_\alpha(\mathbf{q}) = \hat{\mathcal{J}}_\alpha^\dagger(-\mathbf{q})$ it follows that $\left(\hat{\mathcal{J}}_\alpha^{\mathbf{k},-\mathbf{q}}\right)^\dagger = e^{-i(\mathbf{k}-\mathbf{q})\cdot\hat{\mathbf{r}}}\hat{\mathcal{J}}_\alpha(\mathbf{q})e^{i\mathbf{k}\cdot\hat{\mathbf{r}}}$ so that Eq. (20) can be written as

$$\overline{P}_{\alpha,\kappa\beta}^{\mathbf{q}} = \frac{2}{N_k}\sum_{n\mathbf{k}}\left[\langle u_{n\mathbf{k}}|\hat{\mathcal{J}}_\alpha^{\mathbf{k},\mathbf{q}}|\delta u_{n\mathbf{k},\mathbf{q}}^{\kappa\beta}\rangle \right.$$
$$\left. + \langle\delta u_{n\mathbf{k},-\mathbf{q}}^{\kappa\beta}|\left(\hat{\mathcal{J}}_\alpha^{\mathbf{k},-\mathbf{q}}\right)^\dagger|u_{n\mathbf{k}}\rangle\right]. \tag{23}$$

In this work we shall limit our focus to materials with time-reversal symmetry (TRS); then we have

$$\langle\mathbf{s}|u_{n\mathbf{k}}\rangle = \langle u_{n-\mathbf{k}}|\mathbf{s}\rangle, \quad \langle\mathbf{s}|\delta u_{n\mathbf{k},\mathbf{q}}^{\kappa\beta}\rangle = -\langle\delta u_{n-\mathbf{k},-\mathbf{q}}^{\kappa\beta}|\mathbf{s}\rangle, \tag{24}$$

where the negative sign in the second expression is a result of the $-i$ in the first-order adiabatic wavefunction [see Eq. (11)]. Assuming that the current operator has

the correct "TRS odd" nature, i.e., $\left(\langle\mathbf{s}|\hat{\mathcal{J}}_\alpha^{\mathbf{k},-\mathbf{q}}|\mathbf{s}'\rangle\right)^* = -\langle\mathbf{s}|\hat{\mathcal{J}}_\alpha^{-\mathbf{k},\mathbf{q}}|\mathbf{s}'\rangle$, Eq. (23) simplifies to

$$\overline{P}^{\mathbf{q}}_{\alpha,\kappa\beta} = \frac{4}{N_k}\sum_{n\mathbf{k}}\langle u_{n\mathbf{k}}|\hat{\mathcal{J}}_\alpha^{\mathbf{k},\mathbf{q}}|\delta u_{n\mathbf{k},\mathbf{q}}^{\kappa\beta}\rangle. \tag{25}$$

B. Current-density operator

We now consider the form of the current-density operator. If particle density is conserved, any physically meaningful definition of current density must satisfy the continuity condition

$$\nabla\cdot\mathbf{J}(\mathbf{r}) = -\frac{\partial\rho(\mathbf{r})}{\partial t}, \tag{26}$$

where ρ is the particle density. In a quantum mechanical treatment,[25] $\rho(\mathbf{r}) = |\Psi(\mathbf{r})|^2$, where Ψ is the solution to the time-dependent Schrödinger equation. Combining Eq. (9) with its complex conjugate gives

$$\frac{\partial}{\partial t}\rho(\mathbf{r}) = -i\langle\Psi|\left[|\mathbf{r}\rangle\langle\mathbf{r}|,\hat{H}\right]|\Psi\rangle = -i\langle\Psi|\left[\hat{\rho}(\mathbf{r}),\hat{H}\right]|\Psi\rangle, \tag{27}$$

where $\hat{\rho}(\mathbf{r})$ is the particle density operator. (We use atomic units throughout with an electron charge of -1.) In terms of the first-order adiabatic expansion of Eq. (10), we can use Eq. (27) to write the induced density from an adiabatic perturbation parameterized by λ as

$$\rho_\lambda(\mathbf{r}) = -i\left(\langle\psi|\left[\hat{\rho}(\mathbf{r}),\hat{H}\right]|\delta\psi\rangle + \langle\delta\psi|\left[\hat{\rho}(\mathbf{r}),\hat{H}\right]|\psi\rangle\right). \tag{28}$$

1. Local potentials

Consider the simplest case of a Hamiltonian of the form $\hat{H}^{\mathrm{loc}} = \hat{\mathbf{p}}^2/2 + \hat{V}^{\mathrm{loc}}$ where $\hat{\mathbf{p}}$ is the momentum operator and $\hat{V}^{\mathrm{loc}} = \int\hat{\rho}(\mathbf{r})V(\mathbf{r})d^3r$ is a local scalar potential. The local potential commutes with the density operator, so the only contribution to the current is from the momentum operator. Comparing Eqs. (26) and (27) results in the textbook form of the current-density operator

$$\hat{\mathcal{J}}_\alpha^{\mathrm{loc}}(\mathbf{r}) = -\frac{1}{2}\left(|\mathbf{r}\rangle\langle\mathbf{r}|\hat{p}_\alpha + \hat{p}_\alpha|\mathbf{r}\rangle\langle\mathbf{r}|\right)$$
$$= -\frac{1}{2}\left\{\hat{\rho}(\mathbf{r}),\hat{p}_\alpha\right\}. \tag{29}$$

Using Eq. (19), we have

$$\hat{\mathcal{J}}_\alpha^{\mathrm{loc}}(\mathbf{q}) = -\frac{1}{2}\left(e^{-i\mathbf{q}\cdot\hat{\mathbf{r}}}\hat{p}_\alpha + \hat{p}_\alpha e^{-i\mathbf{q}\cdot\hat{\mathbf{r}}}\right), \tag{30}$$

which gives the cell-periodic operator (Appendix A and B)

$$\hat{\mathcal{J}}_\alpha^{\mathbf{k},\mathbf{q},\mathrm{loc}} = -\left(\hat{p}_\alpha^{\mathbf{k}} + \frac{q_\alpha}{2}\right), \tag{31}$$

where $\hat{p}_\alpha^{\mathbf{k}} = -i\hat{\nabla}_\alpha + \hat{k}_\alpha$ is the cell-periodic momentum operator ($\hat{\nabla}_\alpha$ is a spatial derivative in the α direction, and the overall minus sign is from the electron charge).

2. Continuity condition and nonlocal potentials

As mentioned above, *nonlocal* potentials are ubiquitous in modern pseudopotential implementations of DFT.[27–30] When nonlocal potentials are present in the Hamiltonian, the current density in Eq. (29) does not satisfy the continuity equation.

To see this, consider a Hamiltonian with a nonlocal potential: $\hat{H}^{\mathrm{nl}} = \hat{\mathbf{p}}^2/2 + \hat{V}^{\mathrm{loc}} + \hat{V}^{\mathrm{nl}}$ with $\hat{V}^{\mathrm{nl}} = \int d^3r\int d^3r'\hat{\rho}(\mathbf{r},\mathbf{r}')V(\mathbf{r},\mathbf{r}')$ where $\hat{\rho}(\mathbf{r},\mathbf{r}') = |\mathbf{r}\rangle\langle\mathbf{r}'|$. In this case there is a term in the induced density [Eq. (28)] resulting from the nonlocal potential:

$$\rho_\lambda^{\mathrm{nl}}(\mathbf{r}) = -i\Big(\langle\psi|\left[\hat{\rho}(\mathbf{r}),\hat{V}^{\mathrm{nl}}\right]|\delta\psi\rangle$$
$$+ \langle\delta\psi|\left[\hat{\rho}(\mathbf{r}),\hat{V}^{\mathrm{nl}}\right]|\psi\rangle\Big), \tag{32}$$

If we write the total induced current as the sum of contributions from the local and nonlocal parts, $\mathbf{J} = \mathbf{J}^{\mathrm{loc}} + \mathbf{J}^{\mathrm{nl}}$, then we have

$$\nabla\cdot\mathbf{J}^{\mathrm{nl}}(\mathbf{r}) = -\rho_\lambda^{\mathrm{nl}}(\mathbf{r}). \tag{33}$$

This "nonlocal charge," $\rho_\lambda^{\mathrm{nl}}$, measures the degree to which the continuity equation, Eq. (26), breaks down if Eq. (29) is used in a nonlocal pseudopotential context.

Li *et al.*[26] argued that such nonlocal charge could be used to reconstruct the nonlocal contribution to the current density via a Poisson equation. Indeed, Eq. (33) indicates that the irrotational part of $\mathbf{J}^{\mathrm{nl}}$ can be determined by calculating Eq. (32). Their approach yields a conserved current by construction, but there are two additional requirements that a physically meaningful definition of the quantum-mechanical electronic current should satisfy:

- The nonlocality of the Hamiltonian should be confined to small spheres surrounding the ionic cores. In the interstitial regions, the nonlocal part of the pseudopotentials vanish, and the Hamiltonian operator is local therein. Thus, the current-density operator should reduce to the simple textbook formula outside the atomic spheres. The corollary is that $\mathbf{J}^{\mathrm{nl}}(\mathbf{r})$ must vanish in the interstitial regions.

- The macroscopic average of the microscopic current should reduce to the well-known expression $\hat{v}_\alpha = -i[\hat{r}_\alpha,\hat{H}]$ for the electronic velocity operator.[47–50] This is routinely used in the context of DFPT, e.g., to calculate the polarization response to ionic displacements needed for the Born effective charge tensor.

The strategy proposed by Li *et al.*[26] falls short of fulfilling either condition. Regarding the first (spatial confinement), note that the nonlocal charge associated to

individual spheres generally has a nonzero dipole (and higher multipole) moments. Therefore, even if the non-local charge is confined to the sphere, an irrotational field whose divergence results in such a charge density will generally have a long-ranged character and propagate over all space.

Regarding the relation to the macroscopic particle velocity, note that the construction proposed by Li *et al.*[26] in practice discards the solenoidal part of the nonlocal current and hence fails at describing its contribution to the transverse polarization response. This is precisely the quantity in which we are interested in the context of flexoelectricity, and is also crucial for obtaining other important quantities, such as the Born charge tensor, that are part of standard DFPT implementations.

Therefore, a calculation of Eqs. (32) does not contain the necessary information to determine $\mathbf{J}^{\mathrm{nl}}$, and an alternative derivation to the textbook one outlined in Sec. III B 1 is required.

3. Current-density operator generalized for nonlocal potentials

In light of the previous section, we will now focus on determining an expression for $\hat{\mathcal{J}}_\alpha$ that is applicable when nonlocal potentials are present in the Hamiltonian. For the case of a perturbation that is uniform over the crystal, corresponding to the long wavelength $\mathbf{q} = 0$ limit of Eq. (3), it is well known that the momentum operator should be replaced with the canonical velocity operator $\hat{v}_\alpha$[47–50] in order to determine the *macroscopic* current.

In Ref. 31, the expression for the *microscopic* current operator that was used to calculate the current induced by a uniform electric field was Eq. (29) with $\hat{p}_\alpha$ replaced by $\hat{v}_\alpha$. Although this treatment will result in the correct current when averaged over a unit cell, this operator does not satisfy the continuity condition in Eq. (26) except in the special case of a Hamiltonian with only local potentials, where it reduces to Eq. (29).

Since we shall be treating a long wavelength acoustic phonon in this study, and we require the polarization response be correct at least to second order in $\mathbf{q}$ [*cf.* Eq. (7)], we require a version of $\hat{\mathcal{J}}_\alpha$ that is designed to handle spatially varying perturbations. Therefore, for our purposes, we need an alternative starting point for the derivation of a current-density expression, different from the one based on the continuity condition that led to, e.g., Eq. (29).

In general, for an arbitrary electronic Hamiltonian $\hat{H}^{\mathbf{A}}$ coupled to a vector potential $\mathbf{A}(\mathbf{r})$, the most general form for the current-density operator is

$$\hat{\mathcal{J}}_\alpha(\mathbf{r}) = -\frac{\partial \hat{H}^{\mathbf{A}}}{\partial A_\alpha(\mathbf{r})}. \tag{34}$$

Our strategy will be to use a vector potential to probe the response to the strain gradient, which will give us the

current density via Eq. (34). Since we are treating the strain gradient in terms of a long-wavelength acoustic phonon of wavevector $\mathbf{q}$, and we are interested in the response occurring at the same wavevector $\mathbf{q}$, it is useful to define

$$\hat{\mathcal{J}}_\alpha(\mathbf{r}) = \sum_{\mathbf{G}} \hat{\mathcal{J}}_\alpha(\mathbf{G} + \mathbf{q}) e^{i(\mathbf{G}+\mathbf{q}) \cdot \mathbf{r}}, \tag{35}$$

$$A_\alpha(\mathbf{r}) = \sum_{\mathbf{G}} A_\alpha(\mathbf{G} + \mathbf{q}) e^{i(\mathbf{G}+\mathbf{q}) \cdot \mathbf{r}}, \tag{36}$$

$$P_{\alpha,\kappa\beta\mathbf{q}}(\mathbf{r}) = \sum_{\mathbf{G}} P_{\alpha,\kappa\beta\mathbf{q}}(\mathbf{G} + \mathbf{q}) e^{i(\mathbf{G}+\mathbf{q}) \cdot \mathbf{r}}. \tag{37}$$

With these definitions, Eq. (34) becomes

$$\hat{\mathcal{J}}_\alpha(\mathbf{G} + \mathbf{q}) = -\frac{\partial \hat{H}^{\mathbf{A}}}{\partial A_\alpha^*(\mathbf{G} + \mathbf{q})} \tag{38}$$

and the desired operator for Eq. (20) is

$$\hat{\mathcal{J}}_\alpha(\mathbf{q}) = -\frac{\partial \hat{H}^{\mathbf{A}}}{\partial A_\alpha^*(\mathbf{q})}. \tag{39}$$

Again, if the Hamiltonian of interest had the form of $H^{\mathrm{loc}} = (\hat{\mathbf{p}} + \hat{\mathbf{A}})^2/2 + \hat{V}^{\mathrm{loc}}$, where the scalar potential is local and $\hat{\mathbf{A}} = \int \hat{\rho}(\mathbf{r}) \mathbf{A}(\mathbf{r}) d^3 r$ is a local vector potential, then $\hat{\mathcal{J}}_\alpha^{\mathrm{loc}}(\mathbf{r}) = -\frac{1}{2} \left\{ \hat{\rho}(\mathbf{r}), (\hat{p}_\alpha + \hat{A}_\alpha) \right\}$. However, for our implementation, we are considering the case where the potential $\hat{V}$ is nonlocal, so we must determine how to couple a generally nonlocal Hamiltonian to a spatially nonuniform vector potential field (which will be the case for a finite $\mathbf{q}$ perturbation).

The standard strategy for describing the coupling to the vector potential is to multiply the nonlocal operator by a complex phase containing the line integral of the vector potential $\mathbf{A}$;[33,34,51] in the real-space representation:

$$\mathcal{O}^{\mathbf{A}}(\mathbf{s}, \mathbf{s}') = \mathcal{O}(\mathbf{s}, \mathbf{s}') e^{-i \int_{\mathbf{s}' \to \mathbf{s}} \mathbf{A} \cdot d\ell}. \tag{40}$$

The different methods that have been proposed for coupling $\mathbf{A}$ to a nonlocal Hamiltonian amount to applying the complex phase in Eq. (40) to either the entire Hamiltonian[51] or just the nonlocal potential,[33,34] and choosing either a straight-line path[33,51] or a path that passes through the centers of the atoms[34] to perform the line integral.

4. Straight-line path

Using Feynman path integrals, Ismail-Beigi, Chang, and Louie[33] (ICL) derived the following form of a nonlocal Hamiltonian coupled to a vector potential field:

$$\hat{H}_{\mathrm{ICL}}^{\mathbf{A}} = \frac{1}{2} (\hat{\mathbf{p}} + \hat{\mathbf{A}})^2 + \hat{V}^{\mathrm{loc}} + \int d^3 s \int d^3 s' \hat{\rho}(\mathbf{s}, \mathbf{s}') V^{\mathrm{nl}}(\mathbf{s}, \mathbf{s}') e^{-i \int_{\mathbf{s}'}^{\mathbf{s}} \mathbf{A} \cdot d\ell}, \tag{41}$$

where the line integral is taken along a straight path from $\mathbf{s}$ to $\mathbf{s}'$. Since the approach used in Ref. 33 to perform the minimal substitution $\hat{\mathbf{p}} \rightarrow \hat{\mathbf{p}} + \hat{\mathbf{A}}$ is general, applying to both local and nonlocal Hamiltonians, this approach is equivalent to the approach of Essin *et al.*, where the coupled Hamiltonian is written

$$H^{\mathbf{A}}(\mathbf{s}, \mathbf{s}') = H(\mathbf{s}, \mathbf{s}') e^{-i \int_{\mathbf{s}'}^{\mathbf{s}} \mathbf{A} \cdot d\ell}, \qquad (42)$$

i.e., all of the $\mathbf{A}$ dependence is contained in the complex phase, and the line integral is also taken along a straight path from $\mathbf{s}$ to $\mathbf{s}'$.

Expanding Eq. (42) to first order gives

$$H^{\mathbf{A}}(\mathbf{s}, \mathbf{s}') = H(\mathbf{s}, \mathbf{s}') - i H(\mathbf{s}, \mathbf{s}') \int_{\mathbf{s}'}^{\mathbf{s}} \mathbf{A} \cdot d\ell + \cdots. \quad (43)$$

We would like to evaluate Eq. (39) for this form of the Hamiltonian. Since $\mathbf{A}(\mathbf{r})$ is real we can write Eq. (36) as $A_\alpha(\mathbf{r}) = A_\alpha^*(\mathbf{r}) = A_\alpha^*(\mathbf{q}) e^{-i\mathbf{q} \cdot \mathbf{r}}$ so that the integral over $\mathbf{A}$ for the ICL[33] path is

$$\int_{\mathbf{s}'}^{\mathbf{s}} \mathbf{A} \cdot d\ell = \int_0^1 d\tau \mathbf{A}[\mathbf{s}' + \tau(\mathbf{s} - \mathbf{s}')] \cdot (\mathbf{s} - \mathbf{s}')$$

$$= \mathbf{A}^*(\mathbf{q}) \cdot (\mathbf{s} - \mathbf{s}') \int_0^1 d\tau e^{-i\mathbf{q} \cdot [\mathbf{s}' + \tau(\mathbf{s} - \mathbf{s}')]} \quad (44)$$

$$= -\mathbf{A}^*(\mathbf{q}) \cdot (\mathbf{s} - \mathbf{s}') \frac{e^{-i\mathbf{q} \cdot \mathbf{s}} - e^{-i\mathbf{q} \cdot \mathbf{s}'}}{i\mathbf{q} \cdot (\mathbf{s} - \mathbf{s}')}$$

Therefore, from Eqs. (43) and (39),

$$\langle \mathbf{s} | \hat{\mathcal{J}}_\alpha^{\mathrm{ICL}}(\mathbf{q}) | \mathbf{s}' \rangle = -i H(\mathbf{s}, \mathbf{s}')(s_\alpha - s_\alpha') \frac{e^{-i\mathbf{q} \cdot \mathbf{s}} - e^{-i\mathbf{q} \cdot \mathbf{s}'}}{i\mathbf{q} \cdot (\mathbf{s} - \mathbf{s}')}. \tag{45}$$

In practice we shall normally work in terms of the cell-periodic current operator of Eq. (22), whose position representation follows as

$$\langle \mathbf{s} | \hat{\mathcal{J}}_\alpha^{\mathbf{k}, \mathbf{q}, \mathrm{ICL}} | \mathbf{s}' \rangle = -i H^{\mathbf{k}}(\mathbf{s}, \mathbf{s}')(s_\alpha - s_\alpha') \frac{e^{-i\mathbf{q} \cdot (\mathbf{s} - \mathbf{s}')} - 1}{i\mathbf{q} \cdot (\mathbf{s} - \mathbf{s}')}. \tag{46}$$

We can see that the current operator of Eq. (45) satisfies the continuity condition of Eq. (26) as follows. In reciprocal space the continuity equation becomes $i\mathbf{q} \cdot [-\hat{\mathcal{J}}^{\mathrm{ICL}}(\mathbf{q})] = -\partial \hat{\rho}_{\mathbf{q}} / \partial t$, where $\hat{\rho}_{\mathbf{q}} = e^{-i\mathbf{q} \cdot \hat{\mathbf{r}}}$ is the $\mathbf{G} = 0$ particle density operator for a given $\mathbf{q}$, and the negative sign in front of the current operator reflects the sign of the electron charge. But from Eq. (45) it quickly follows that

$$-i\mathbf{q} \cdot \langle \mathbf{s} | \hat{\mathcal{J}}_\alpha^{\mathrm{ICL}}(\mathbf{q}) | \mathbf{s}' \rangle = i \langle \mathbf{s} | \left[\hat{\rho}_{\mathbf{q}}, \hat{H} \right] | \mathbf{s}' \rangle \qquad (47)$$

which, using the Ehrenfest theorem, is nothing other than $-\partial \hat{\rho}_{\mathbf{q}} / \partial t$ in the position representation.

In the case that only local potentials are present, only the kinetic term in the Hamiltonian contributes to $\hat{\mathcal{J}}_\alpha^{\mathrm{ICL}}(\mathbf{q})$. We show in Appendix A that the current operator then reduces to the form of Eq. (30). The fact that the local and nonlocal parts can be separated confirms the equivalence of the ICL [Eq. (41)] and Essin *et al.* [Eq. (42)] approaches.

In the case that nonlocal potentials are present, we show in Appendix A that, for $\mathbf{q} = 0$, Eq. (45) reduces to the well-known expression for the canonical velocity operator[47–50] $\hat{\mathcal{J}}_\alpha^{\mathrm{ICL}}(\mathbf{q} = 0) = -\hat{v}_\alpha = i \left[\hat{r}_\alpha, \hat{H} \right]$, where the -1 comes from the electron charge. We discuss the case of nonlocal potentials and finite $\mathbf{q}$ perturbations in Sec. III C.

5. Path through atom center

Subsequently, Pickard and Mauri[34] (PM) proposed using a path from $\mathbf{s}$ to the atom center, $\mathbf{R}$, and then to $\mathbf{s}'$, which was constructed explicitly to give better agreement for magnetic susceptibility between pseudopotential and all-electron calculations. This approach can be regarded as a generalization to spatially nonuniform fields of the gauge-including projector augmented-wave (GIPAW) method,[34,37] where the PAW transformation is modified with a complex phase in order to ensure that the pseudowavefunction has the correct magnetic translational symmetry.

The coupled Hamiltonian used in Ref. 34 is of the form

$$\hat{H}_{\mathrm{PM}}^{\mathbf{A}} = \frac{1}{2}(\hat{\mathbf{p}} + \hat{\mathbf{A}})^2 + \hat{V}^{\mathrm{loc}} + \sum_{\zeta=1}^{N} \int d^3 s \int d^3 s'$$
$$\times \hat{\rho}(\mathbf{s}, \mathbf{s}') V_\zeta^{\mathrm{nl}}(\mathbf{s}, \mathbf{s}') e^{-i \int_{\mathbf{s}' \rightarrow \mathbf{R}_\zeta \rightarrow \mathbf{s}} \mathbf{A} \cdot d\ell}, \qquad (48)$$

where N is the number of atoms in the cell, $\mathbf{R}_\zeta$ is the position of atom ζ, and V_ζ^{nl} is the nonlocal potential for that atom. The PM approach explicitly splits the nonlocal contribution from $\mathbf{A}$ into contributions from each atomic sphere centered at $\mathbf{R}_\zeta$.[52] Therefore, the total current operator is

$$\hat{\mathcal{J}}_\alpha^{\mathbf{k}, \mathbf{q}, \mathrm{PM}} = - \left(\hat{p}_\alpha^{\mathbf{k}} + \frac{q_\alpha}{2} \right) + \sum_{\zeta=1}^{N} \hat{\mathcal{J}}_{\alpha, \zeta}^{\mathbf{k}, \mathbf{q}, \mathrm{PM}, \mathrm{nl}}, \qquad (49)$$

where the superscript "nl" and the subscript ζ emphasize that each item in the summation describes the contribution to the current from the nonlocal potential of the atom ζ; it is obvious from Eqs. (48) and (49) that $\hat{\mathcal{J}}_\alpha^{\mathrm{loc}}$ will be recovered in the case of a local potential.

For an atom at position $\mathbf{R}_\zeta$, the line integral in Eq. (48) is

$$\int_{\mathbf{s}'\to\mathbf{R}_\zeta\to\mathbf{s}} \mathbf{A}\cdot d\ell = -\mathbf{A}^*(\mathbf{q})\cdot(\mathbf{R}_\zeta-\mathbf{s}')\frac{e^{-i\mathbf{q}\cdot\mathbf{R}_\zeta}-e^{-i\mathbf{q}\cdot\mathbf{s}'}}{i\mathbf{q}\cdot(\mathbf{R}_\zeta-\mathbf{s}')} - \mathbf{A}^*(\mathbf{q})\cdot(\mathbf{s}-\mathbf{R}_\zeta)\frac{e^{-i\mathbf{q}\cdot\mathbf{s}}-e^{-i\mathbf{q}\cdot\mathbf{R}_\zeta}}{i\mathbf{q}\cdot(\mathbf{s}-\mathbf{R}_\zeta)}. \tag{50}$$

Therefore we have

$$\langle\mathbf{s}|\hat{\mathcal{J}}_{\alpha,\zeta}^{\mathrm{PM,nl}}(\mathbf{q})|\mathbf{s}'\rangle = -iV_\zeta^{\mathrm{nl}}(\mathbf{s},\mathbf{s}')\left[(R_{\alpha,\zeta}-s'_\alpha)\frac{e^{-i\mathbf{q}\cdot\mathbf{R}_\zeta}-e^{-i\mathbf{q}\cdot\mathbf{s}'}}{i\mathbf{q}\cdot(\mathbf{R}_\zeta-\mathbf{s}')} + (s_\alpha-R_{\alpha,\zeta})\frac{e^{-i\mathbf{q}\cdot\mathbf{s}}-e^{-i\mathbf{q}\cdot\mathbf{R}_\zeta}}{i\mathbf{q}\cdot(\mathbf{s}-\mathbf{R}_\zeta)}\right], \tag{51}$$

so the cell-periodic operator is

$$\langle\mathbf{s}|\hat{\mathcal{J}}_{\alpha,\zeta}^{\mathbf{k},\mathbf{q},\mathrm{PM,nl}}|\mathbf{s}'\rangle = -iV_\zeta^{\mathrm{nl}}(\mathbf{s},\mathbf{s}')\left[(R_{\alpha,\zeta}-s'_\alpha)\frac{e^{-i\mathbf{q}\cdot(\mathbf{R}_\zeta-\mathbf{s}')}-1}{i\mathbf{q}\cdot(\mathbf{R}_\zeta-\mathbf{s}')} + (s_\alpha-R_{\alpha,\zeta})\frac{e^{-i\mathbf{q}\cdot(\mathbf{s}-\mathbf{s}')}-e^{-i\mathbf{q}\cdot(\mathbf{R}_\zeta-\mathbf{s}')}}{i\mathbf{q}\cdot(\mathbf{s}-\mathbf{R}_\zeta)}\right]. \tag{52}$$

From Eqs. (51) and (32), we see that $i\mathbf{q}\cdot[-\hat{\mathcal{J}}^{\mathrm{PM,nl}}(\mathbf{q})] = i\left[e^{-i\mathbf{q}\cdot\hat{\mathbf{r}}},\hat{V}^{\mathrm{nl}}\right] = -\hat{\rho}_\lambda^{\mathrm{nl}}$. Therefore, Eq. (49) satisfies the continuity condition. Also, in the case of a $\mathbf{q}=0$ perturbation, $\hat{\mathcal{J}}_\alpha^{\mathrm{PM,nl}}(\mathbf{q}=0) = i\left[\hat{r}_\alpha,\hat{V}^{\mathrm{nl}}\right]$, which is the nonlocal contribution to $-\hat{v}_\alpha$, as expected. We discuss the case of nonlocal potentials and finite $\mathbf{q}$ perturbations in the next section.

Finally, we see that for the longitudinal response (where $\mathbf{q}=q_\alpha\hat{\alpha}$), the ICL and PM approaches produce identical operators. This is expected, since they both satisfy the continuity equation. Only circulating currents (e.g., transverse or shear FxE components) may exhibit path dependence.

C. Long wavelength expansion

Recall that only the induced polarization up to second order in $\mathbf{q}$ is required for the FxE coefficients [cf. Eq. (7)]. Therefore, instead of attempting to calculate Eq. (25) with either Eq. (46) or (49) directly, we will expand these expressions for the current-density operator to second order in $\mathbf{q}$.

Considering the Hamiltonian in Eq. (14), there are contributions to $\hat{\mathcal{J}}_\alpha^{\mathbf{q}}$ from the kinetic energy and nonlocal part of the pseudopotential. We show in Appendix A [Eq. (A4)] that the kinetic energy only contributes up to first order in $\mathbf{q}$, and for a local Hamiltonian, the current operator reduces to the form of Eq. (31).

The nonlocal potential will, however, contribute at all orders. As mentioned in Sec. III B 4 and III B 5, for $\mathbf{q}=0$, both the ICL and PM approaches give $\hat{\mathcal{J}}_\alpha^{\mathbf{k},\mathbf{q}=0} = -\hat{v}_\alpha^{\mathbf{k}} = i[\hat{r}_\alpha,\hat{H}^{\mathbf{k}}] = -\hat{p}_\alpha^{\mathbf{k}}+\hat{\mathcal{J}}_\alpha^{\mathbf{k},\mathrm{nl}(0)}$, where we have defined $\hat{\mathcal{J}}_\alpha^{\mathbf{k},\mathrm{nl}(0)} \equiv i[\hat{r}_\alpha,\hat{V}^{\mathbf{k},\mathrm{nl}}]$. At higher orders in $\mathbf{q}$, and for nonlongitudinal response, the ICL and PM approaches may no longer agree.

Up to second order in $\mathbf{q}$, the current operator can be

written as

$$\hat{\mathcal{J}}_\alpha^{\mathbf{k},\mathbf{q}} \simeq -\left(\hat{p}_\alpha^{\mathbf{k}}+\frac{q_\alpha}{2}\right) + \hat{\mathcal{J}}_\alpha^{\mathbf{k},\mathrm{nl}(0)} \\ + \frac{q_\gamma}{2}\hat{\mathcal{J}}_{\alpha,\gamma}^{\mathbf{k},\mathrm{nl}(1)} + \frac{q_\gamma q_\xi}{6}\hat{\mathcal{J}}_{\alpha,\gamma\xi}^{\mathbf{k},\mathrm{nl}(2)}. \tag{53}$$

where the higher order terms in $\mathbf{q}$, $\hat{\mathcal{J}}_{\alpha,\gamma}^{\mathbf{k},\mathbf{q},\mathrm{nl}(1)}$ and $\hat{\mathcal{J}}_{\alpha,\gamma\xi}^{\mathbf{k},\mathbf{q},\mathrm{nl}(2)}$, are the result of the nonlocal part of the Hamiltonian *and* the fact that the monochromatic perturbation is nonuniform (i.e, finite $\mathbf{q}$). Expressions for these last two terms in Eq. (53) are derived in Appendix C for the ICL path [Eqs. (C9) and (C10)] and PM path [Eqs. (C12) and (C13)].

Plugging the current operator from Eq. (53) into Eq. (25), readily yields the induced polarization,

$$\overline{P}_{\alpha,\kappa\beta}^{\mathbf{q}} = \overline{P}_{\alpha,\kappa\beta}^{\mathbf{q},\mathrm{loc}} + \overline{P}_{\alpha,\kappa\beta}^{\mathbf{q},\mathrm{nl}}, \tag{54}$$

where we have separated the contribution of the local current operator (loc) from the nonlocal (nl) part. The exact expression for $\overline{P}_{\alpha,\kappa\beta}^{\mathbf{q},\mathrm{loc}}$ is derived in Appendix B, yielding Eq. (B8); the approximate (exact only up to second order in $\mathbf{q}$) expression for $\overline{P}_{\alpha,\kappa\beta}^{\mathbf{q},\mathrm{nl}}$ is derived in Appendix C [see Eq. (C1)].

D. Circulating rotation-gradient contribution and diamagnetic susceptibility

Transverse or shear strain gradients result in rigid rotations of unit cells which must be treated carefully in order to calculate physically meaningful values of the flexoelectric tensor. This issue can be loosely compared to the well-known distinction between the proper and improper piezoelectric tensor,[53,54] but, in the case of strain gradients, it is complicated by the fact that different parts of the sample typically rotate by different amounts. The reader is referred to Ref. 24 for a complete discussion; only the results of that work necessary for our purposes will be reproduced here.

Larmor's theorem states that the effects of a uniform rotation and those of a uniform magnetic field are the same to first order in the field/angular velocity. Therefore, the local rotations of the sample dynamically produce circulating diamagnetic currents that will contribute to the bulk flexoelectric coefficients as defined in Eq. (7). As was shown in Ref. 24 (see also Appendix D for an abridged derivation), this circulating rotation-gradient (CRG)[55] contribution only concerns the nonlongitudinal components and is proportional to the diamagnetic susceptibility of the material, $\chi_{\gamma\lambda} = \partial M_\gamma / \partial H_\lambda$, where M is the magnetization and H the magnetic field. Specifically,

$$\overline{P}_{\alpha,\beta}^{(2,\omega\nu),\text{CRG}} = \sum_{\gamma\lambda} \left(\epsilon^{\alpha\omega\gamma}\epsilon^{\beta\lambda\nu} + \epsilon^{\alpha\nu\gamma}\epsilon^{\beta\lambda\omega} \right) \chi_{\gamma\lambda}, \quad (55)$$

where ϵ's are Levi-Civita symbols.

The CRG contribution represents a physical response of the bulk material to the rotations resulting from such nonlongitudinal strain gradients. However, in the context of calculating FxE coefficients, it is useful to remove this contribution. The reasoning for doing this is based on the fact that, as shown in Ref. 24, the diamagnetic circulating currents from the CRG contribution are divergentless, and therefore do not result in a build up of charge density anywhere in the crystal. Therefore, for the experimentally relevant case of a *finite* crystal, where the polarization response is completely determined by the induced charge density, the CRG contribution will not produce an electrically measurable response.

The fact that the CRG does contribute to the bulk FxE coefficients, but not to the measurable response of a finite sample, highlights the fact that, for flexoelectricity, the bulk and surface response are intertwined.[19,24,56] Indeed, it was determined in Ref. 24 that there is a surface CRG contribution that will exactly cancel the bulk one [Eq. (55)]. Thus removing the CRG contribution from the bulk coefficients simply corresponds to a different way of partitioning the response between the bulk and the surface. In this work we are focused on the bulk response, and are free to choose a convention for this partition. In order to make a more direct connection with experiments, and to be able to directly compare with charge-density-based calculations,[19] we choose to remove the CRG contribution from our calculated $\overline{P}_{\alpha,\kappa\beta}^{(2,\omega\nu)}$.

To calculate $\chi_{\gamma\lambda}$, there is again a subtlety involved in the use of nonlocal pseudopotentials. Conventional calculations of the diamagnetic susceptibility involve applying a vector potential perturbation and calculating the current response.[32–35,37] In the case of a local Hamiltonian the aforementioned rotational field is indistinguishable from an electromagnetic vector potential, and the expression for $\chi_{\gamma\lambda}$ is identical to the diamagnetic susceptibility. However, in the case of a nonlocal Hamiltonian this is no longer true. In that case, the perturbation remains the *local* current operator, $\hat{\mathcal{J}}^{\text{loc}}$, while the current response is evaluated using the total (local plus nonlocal) $\hat{\mathcal{J}}$ (*cf.* Appendix D). This difference indicates that Larmor's theorem may break down for nonlocal potentials. This is discussed further in Sec. VI.

IV. IMPLEMENTATION

The procedure for calculating the FxE coefficients using the formalism in Sec. III is as follows. We first perform conventional DFPT phonon calculations [displacing sublattice κ in direction β, as in Eq. (3)] at small but finite wavevectors $\mathbf{q}$ to obtain the static first-order wave-functions $|\partial_\lambda u_{n\mathbf{k},\mathbf{q}}^{\kappa\beta}\rangle$. We choose $|q| < 0.04$, where here and henceforth we express q in reduced units of $2\pi/a$ (a is the cubic lattice constant). To avoid the sum over empty states in Eq. (11), we determine the first-order adiabatic wavefunctions by solving the Sternheimer equation

$$(H_\mathbf{k} - \epsilon_{n\mathbf{k}})|\delta u_{n\mathbf{k},\mathbf{q}}^{\kappa\beta}\rangle = -i\mathcal{Q}_{c,\mathbf{k}+\mathbf{q}}|\partial_\lambda u_{n\mathbf{k},\mathbf{q}}^{\kappa\beta}\rangle \quad (56)$$

where $\epsilon_{n\mathbf{k}}$ is the eigenvalue of band n and k-point $\mathbf{k}$ and $\mathcal{Q}_{c,\mathbf{k}+\mathbf{q}}$ is the projector over conduction band states (implemented as one minus the projector over valence states). Then we apply the current operator in Eq. (53) to obtain $\overline{P}_{\alpha,\kappa\beta}^{\mathbf{q}}$ from Eq. (25) (see Appendix B and C for details).

As will be discussed in Sec. V A, we will use the ICL path for most of the calculations in this study, so the explicit expression for this case is provided in this section. The local contribution to $\overline{P}_{\alpha,\kappa\beta}^{\mathbf{q}}$ is derived in Appendix B, leading to Eq. (B8). The three terms in the small-$\mathbf{q}$ expansion of the nonlocal part are determined in Appendix C 1 by combining Eqs. (46) and (25), and expanding in powers of $\mathbf{q}$, leading to Eq. (C1). Combining Eq. (C1) with Eqs. (C8)-(C10) and adding Eq. (B8), we have

$$\overline{P}_{\alpha,\kappa\beta}^{\mathbf{q},\text{ICL}} = -\frac{4}{N_k} \sum_{n\mathbf{k}} \left[\langle u_{n\mathbf{k}}|\hat{p}_\alpha^\mathbf{k} + \frac{q_\alpha}{2}|\delta u_{n\mathbf{k},\mathbf{q}}^{\kappa\beta}\rangle + \langle u_{n\mathbf{k}}|\frac{\partial \hat{V}^{\mathbf{k},\text{nl}}}{\partial k_\alpha}|\delta u_{n\mathbf{k},\mathbf{q}}^{\kappa\beta}\rangle \right.$$
$$\left. + \frac{1}{2}\sum_{\gamma=1}^3 q_\gamma \langle u_{n\mathbf{k}}|\frac{\partial^2 \hat{V}^{\mathbf{k},\text{nl}}}{\partial k_\alpha \partial k_\gamma}|\delta u_{n\mathbf{k},\mathbf{q}}^{\kappa\beta}\rangle + \frac{1}{6}\sum_{\gamma=1}^3\sum_{\xi=1}^3 q_\gamma q_\xi \langle u_{n\mathbf{k}}|\frac{\partial^3 \hat{V}^{\mathbf{k},\text{nl}}}{\partial k_\alpha \partial k_\gamma \partial k_\xi}|\delta u_{n\mathbf{k},\mathbf{q}}^{\kappa\beta}\rangle \right], \quad (57)$$

where we have again assumed TRS [*cf.* Eq. 25]. A simi-
lar equation can be obtained for the PM path using the

first- and second-order current operators derived in Appendix C 2 [Eqs. (C12) and (C13)].

In order to obtain $\overline{P}^{(2,\omega\nu)}_{\alpha,\kappa\beta}$, we calculate numerical second derivatives with respect to q_ω and q_ν yielding the needed flexoelectric coefficients $\mu^{\mathrm{I}}_{\alpha\beta,\omega\nu}$ via Eq. (7). Note that, in addition to the explicit factors of q multiplying the last two terms, each term has an implicit q dependence through $\delta u^{\kappa\beta}_{n\mathbf{k},\mathbf{q}}$ so all terms may contribute to the second derivative.

Since we will consider cubic materials there are three independent FxE coefficients:[15,17]

$$\begin{aligned}
\mu_{\mathrm{L}} &= \mu^{\mathrm{II}}_{11,11} = \mu^{\mathrm{I}}_{11,11}, \\
\mu_{\mathrm{S}} &= \mu^{\mathrm{II}}_{12,12} = \mu^{\mathrm{I}}_{11,22}, \\
\mu_{\mathrm{T}} &= \mu^{\mathrm{II}}_{11,22} = 2\mu^{\mathrm{I}}_{12,12} - \mu^{\mathrm{I}}_{11,22},
\end{aligned} \tag{58}$$

where L stands for longitudinal, S for shear, and T for transverse.

A. Electrostatic boundary conditions

The current response to a phonon perturbation, just like other response properties, displays a strongly nonanalytic behavior in a vicinity of the Γ point ($\mathbf{q} = 0$), so some care is required when taking the long-wavelength expansions described in the previous Sections. A long-wavelength phonon naturally imposes "mixed" electrical (ME) boundary conditions:[17] Along the longitudinal direction ($\hat{\mathbf{q}}$) the electric displacement field, $\mathbf{D}$, must vanish ($\mathbf{D} \cdot \hat{\mathbf{q}} = 0$); conversely, periodicity is preserved in the planes that are normal to $\hat{\mathbf{q}}$, resulting in a vanishing electric field therein. In general, the bulk FxE tensor needs to be defined under isotropic "short-circuit" (SC) boundary conditions, which implies that the problematic longitudinal $\mathbf{E}$-fields must be suppressed. In our calculations, this goal can be achieved using the procedure of Refs. 15 and 19, where the $\mathbf{G} = 0$ component of the self-consistent first-order potential is removed in the DFPT calculation of $\partial_\lambda u^{\kappa\beta}_{n\mathbf{k},\mathbf{q}}$ [Eq. (56)]. We will use this procedure for the calculations of cubic oxides in Sec. V B.

For several reasons, one may sometimes be interested in calculating the flexoelectric coefficients under mixed electrical boundary conditions; in such a case, of course, the $\mathbf{G} = 0$ component of the self-consistent first-order potential should not be removed. Then, however, one must keep in mind that the long-wavelength expansion of the polarization response is only allowed along a fixed direction in reciprocal space. (This implies performing the calculations at points $\mathbf{q} = q\hat{\mathbf{q}}$, and subsequently operating the Taylor expansion as a function of the one-dimensional parameter q.) In crystals where the macroscopic dielectric tensor is isotropic and $\hat{\mathbf{q}}$ corresponds to a high-symmetry direction, the longitudinal coefficients for mixed electrical boundary conditions are simply related to the short circuit ones by the dielectric constant, ϵ,

$$\mu^{\mathrm{SC}}_{\mathrm{L}} = \epsilon\mu^{\mathrm{ME}}_{\mathrm{L}}. \tag{59}$$

We will use mixed electrical boundary conditions for our benchmark calculations of noble gas atoms in Sec. V A since, in this particular system, $\mu^{\mathrm{ME}}_{\mathrm{L}}$, rather than $\mu^{\mathrm{SC}}_{\mathrm{L}}$, can be directly compared to the moments of the real-space charge density,[17] as discussed in Sec. V A 1.

B. Magnetic susceptibility contribution

In Sec. III D, we explained that the diamagnetic susceptibility is required in order to correct for the CRG contribution to the FxE coefficients. To avoid the sum over states in Eq. (D3), we solve the Sternheimer equation

$$(\hat{H}_\mathbf{k} - \epsilon_{n\mathbf{k}})|\partial_{\dot{\alpha}} u^\alpha_{n\mathbf{k},\mathbf{q}}\rangle = \mathcal{Q}_{c,\mathbf{k}+\mathbf{q}}\left(\hat{p}^\mathbf{k}_\alpha + \frac{q_\alpha}{2}\right)|u_{n\mathbf{k}}\rangle. \tag{60}$$

Recall that $-\left(\hat{p}^\mathbf{k}_\alpha + \hat{q}_\alpha/2\right)$ is the cell-averaged current operator in the case of a local potential. We then apply the *full* current operator [Eq. (53)] to obtain Eq. (D4) at several small but finite q (as above, $|q| < 0.04$) in order to perform a numerical second derivative and obtain $\overline{P}^{(2,\omega\nu),\,\mathrm{CRG}}_{\alpha,\beta}$ from Eq. (55).

For the case of a material with cubic symmetry, where $\chi_{\alpha\beta} = \chi_{\mathrm{mag}}\delta_{\alpha\beta}$, we see from Eq. (55) that there will be two nonzero elements of the CRG contribution: $\overline{P}^{(2,22),\,\mathrm{CRG}}_{1,1} = 2\chi_{\mathrm{mag}}$ and $\overline{P}^{(2,12),\,\mathrm{CRG}}_{1,2} = -\chi_{\mathrm{mag}}$. Therefore, the CI FxE constants with the CRG contribution removed, μ', are given by[24]

$$\begin{aligned}
\mu'_{\mathrm{L}} &= \mu_{\mathrm{L}}, \\
\mu'_{\mathrm{S}} &= \mu_{\mathrm{S}} - \chi_{\mathrm{mag}}, \\
\mu'_{\mathrm{T}} &= \mu_{\mathrm{T}} + 2\chi_{\mathrm{mag}},
\end{aligned} \tag{61}$$

for cubic materials.

C. Rigid-core correction

It was demonstrated in Ref. 16 that the CI FxE constants depend on the treatment of the core density, which will be different for a different choice of pseudopotential. This dependence is exactly canceled when the surface contribution is calculated consistently with the same pseudopotentials.[21,56] In order to report more "portable" values for the bulk FxE coefficients, we apply the rigid-core correction (RCC) of Refs. 16 and 17:

$$Q^{\mathrm{RCC}}_\kappa = 4\pi \int dr\, r^4 \left[\rho^{\mathrm{AE}}_\kappa(\mathbf{r}) - \rho^{\mathrm{PS}}_\kappa(\mathbf{r})\right], \tag{62}$$

where $\rho^{\mathrm{AE}}_\kappa(r)$ is the all-electron density of the free atom of type κ, and $\rho^{\mathrm{PS}}_\kappa(r)$ is the corresponding pseudocharge density. In Table I we list Q^{RCC} for the various atoms

TABLE I. Q^{RCC} for the various atoms in the materials in Sec. V B in units of e Bohr^2.

	Q^{RCC}		Q^{RCC}
Sr	-5.93	Ba	-13.39
Ti	-0.54	Zr	-4.55
O	-0.01	Pb	-15.16
Mg	-4.85		

that we will require for the cubic oxides reported below (no RCC is included for the noble gas atoms in Sec. V A). Specifically, for short circuit boundary conditions, $\epsilon \sum_\kappa Q_\kappa^{\text{RCC}}/6\Omega$ must be added to μ_{L} and μ_{T}.[56]

D. Computational details

We have implemented the procedure for calculating the FxE coefficients in the ABINIT code.[57] The PBE generalized gradient approximation functional[58] is used throughout. The conventional phonon and dielectric constant calculations are carried out using the DFPT implementation available in the code.[59,60] In order to solve the non-selfconsistent Sternheimer Eqs. (60) and (56), ABINIT's implementation of the variational approach of Ref. 44 is used.

The nuclei and core electrons are described with optimized norm-conserving Vanderbilt pseudopotentials[61] provided by ABINIT. For the cubic oxides, an $8 \times 8 \times 8$ Monkhorst-Pack[62] k-point mesh is used to sample the Brillouin zone, and the plane-wave energy cutoff is set of 60 Ha. For the isolated atoms, a $2 \times 2 \times 2$ k-point mesh is used, and the plane-wave energy cutoff is set of 70 Ha.

V. RESULTS

A. Benchmark test: Isolated noble gas atoms

1. Isolated rigid charge model

In order to test the implementation described in Sec. IV, we consider the toy model of a material made of rigid noninteracting spherical charge distributions arranged in a simple cubic lattice, as explored in Refs. 24, 21, and 56. We shall refer to this henceforth as the "isolated rigid charge" (IRC) model. Of course, such a material is fictitious, since it would have no interatomic forces to hold it together; even so, it serves as an interesting test case since its FxE properties can be determined analytically and compared to our numerical calculations. In this section, we will briefly summarize the expectations of the IRC model (see Refs. 24 and 21 for a more complete discussion).

For the IRC "material," there is only one sublattice per cell. Each "atom" is represented by a spherically symmetric charge density $\rho_{\text{IRC}}(r)$ that falls to zero beyond a

cutoff r_c chosen small enough to insure that the atomic spheres do not overlap. The atoms are assumed to be neutral, $\int_0^{r_c} \rho_{\text{IRC}}(r)\, r^2\, dr = 0$. It was shown in Ref. 24 that the longitudinal and shear coefficients for the IRC model calculated from the induced current-density are

$$\mu_{\text{L,IRC}} = \mu_{\text{S,IRC}} = \frac{Q_{\text{IRC}}}{2\Omega}, \qquad (63)$$

where $\Omega = a^3$ is the cell volume, and

$$Q_{\text{IRC}} = \int d^3r\, \rho_{\text{IRC}}(r)x^2 \qquad (64)$$

is the quadrupolar moment of the atomic charge density (of course the direction x is arbitrary since the charge density is spherically symmetric).

The FxE constants in Eq. (63) include the CRG contribution to the current discussed in Sec. III D.[19,24,56] Removing this contribution from our bulk coefficients [see Eq. (61)] results in the primed coefficients for the IRC model[24]

$$\mu'_{\text{L,IRC}} = \frac{Q_{\text{IRC}}}{2\Omega}, \quad \mu'_{\text{S,IRC}} = 0, \qquad (65)$$

where the CRG contribution is given by

$$\chi_{\text{mag,IRC}} = \mu_{\text{S,IRC}} = \frac{Q_{\text{IRC}}}{2\Omega} \qquad (66)$$

If we assume that Larmor's theorem holds (i.e., that the CRG contribution is identical to the magnetic susceptibility), Eq. (66) is just a statement of the Langevin theory of diamagnetism, which relates the magnetic susceptibility to the quadrupole moment of a spherical atomic charge (see Sec. VI).

2. Noble gas atoms

In the following subsections (V A 3, V A 4, V A 5), we will compare the behavior of this model with the results of DFT calculations on isolated noble gas atoms. Several points should be considered when comparing the results of such calculations to the expectations of the IRC model (relations in Sec. V A 1).

Firstly, the noble gas atoms in our DFT calculations are slightly polarizable, i.e., not perfectly described by rigid charge densities. For this reason the longitudinal FxE coefficient will depend on the choice of electrostatic boundary conditions (see Sec. IV A). We will use mixed electrical boundary conditions, where we should find [analogously to Eq. (63)]

$$\mu_{\text{L,NG}}^{\text{ME}} = \frac{Q_{\text{NG}}}{2\Omega}, \qquad (67)$$

where the subscript "NG" indicates a DFT calculation on a noble gas atom, and Q_{NG} is the quadropole moment of the unperturbed, ground-state charge density of

the noble gas atom. If we had used short circuit boundary conditions, there would have been a factor of ϵ on the right-hand side of Eq. (67). Of course, in the IRC model, the "atoms" are neutral, rigid, and spherical, so $\epsilon = 1$, and, from Eq. (59), short circuit and mixed electric boundary conditions give the same FxE coefficients.

Also, since our noble-gas-atom calculations will use nonlocal pseudopotentials, the equality of $\mu_{\mathrm{S,NG}}$ and $Q_{\mathrm{NG}}/2\Omega$ is not guaranteed; in fact, we will see in Sec. V A 5 that they are not equal. This will be discussed further in Sec. VI in the context of the expected symmetry of the charge response. Similarly, we will find that χ_{mag} does not equal $Q_{\mathrm{NG}}/2\Omega$ [cf. Eq. (66)], indicating that Larmor's theorem breaks down for our form of the current in the presence of nonlocal pseudopotentials (discussed in Sec. VI).

Note that, as with the IRC model, we will drop the κ subscript when discussing the noble gas atoms since the "crystals" that we are considering have only a single sublattice. Also, as all calculations will use mixed electrical boundary condition, we will drop the explicit "ME" labels.

3. Computational strategy: Real-space moments of the charge density

In addition to the relations in Eqs. (63), (65), and (66) of Sec. V A 1 and Eq. (67) of Sec. V A 2, we can perform specific tests of the components of our implementation by exploiting the correspondence between two methods of calculating the FxE coefficients: (i) the long-wavelength expansion in reciprocal space of the polarization induced by a phonon [i.e., Eq. (7)] that we have described so far in this work, and (ii) the computation of the real-space moments of the induced microscopic polarization or charge density from the displacement of an isolated atom in a crystal.[15,17] For the case of the isolated noble gas atoms, displacing the entire sublattice (i.e., applying a $\mathbf{q}=0$ acoustic phonon perturbation) is equivalent to displacing a single atom.

It is particularly useful to compare our methodology to the real-space moments of the induced charge density, since they can be readily calculated from a conventional, DFPT phonon calculation (with $\mathbf{q} = 0$). Specifically, the longitudinal noble-gas response in direction α is[15,17]

$$\mu_{\mathrm{L,NG}} = -\frac{1}{2}\frac{\partial^2 \overline{P}^{\mathbf{q},\mathrm{NG}}_{\alpha,\alpha}}{\partial q_\alpha^2}\bigg|_{\mathbf{q}=0} = \frac{1}{6\Omega}\int_{\mathrm{cell}} d^3 r \rho^{\mathrm{NG}}_{\alpha\mathbf{q}=0}(\mathbf{r}) r_\alpha^3. \tag{68}$$

where $\rho^{\mathrm{NG}}_{\alpha\mathbf{q}}(\mathbf{r}) \equiv \partial\rho^{\mathrm{NG}}(\mathbf{r})/\partial\lambda_{\alpha\mathbf{q}}$ is the first-order induced charge density from a phonon with wavevector $\mathbf{q}$ and noble gas atoms displaced in the α direction. $\overline{P}^{\mathbf{q}}_{\alpha,\alpha}$ is calculated with mixed electrical boundary conditions. As mentioned in Sec. V A 2, the right-hand side of Eq. (68) equals $Q_{\mathrm{NG}}/2\Omega$. Recall that, since the charge density is related to the divergence of the polarization, it only

gives the longitudinal FxE coefficient. Therefore, we can only use an expression like the one in Eq. (68) to test our implementation of μ_{L}.

In general (i.e., not specific to the case of the isolated noble gas atoms), the induced charge density can be split into contributions from the local and nonlocal parts of the Hamiltonian, as we did for the polarization in Eq. (54). Using the continuity condition, we can write the first-order charge as

$$\rho_{\alpha\mathbf{q}}(\mathbf{G}+\mathbf{q}) = -i(\mathbf{G}+\mathbf{q})\cdot\mathbf{P}^{\mathrm{loc}}_{\alpha\mathbf{q}}(\mathbf{G}+\mathbf{q})+\rho^{\mathrm{nl}}_{\alpha\mathbf{q}}(\mathbf{G}+\mathbf{q}). \tag{69}$$

Here $\mathbf{P}^{\mathrm{loc}}_{\alpha\mathbf{q}}$ is the "local" part of the induced polarization and $\rho^{\mathrm{nl}}_{\alpha\mathbf{q}}$ is the nonlocal charge introduced in Sec. III B 2. Using the reciprocal-space version of Eq. (29), the local induced polarization is (assuming TRS)

$$P^{\mathrm{loc}}_{\alpha,\alpha\mathbf{q}}(\mathbf{G}+\mathbf{q}) = -\frac{2}{N_k}\sum_{n\mathbf{k}}\langle\psi_{n\mathbf{k}}|\left\{e^{-i(\mathbf{G}+\mathbf{q})\cdot\hat{\mathbf{r}}}, \hat{p}_\alpha\right\}|\delta\psi^\alpha_{n\mathbf{k},\mathbf{q}}\rangle \tag{70}$$

and the nonlocal charge density from Eq. (32) is given (in reciprocal space) by

$$\rho^{\mathrm{nl}}_{\alpha\mathbf{q}}(\mathbf{G}+\mathbf{q}) = -\frac{4i}{N_k}\sum_{n\mathbf{k}}\langle\psi_{n\mathbf{k}}|\left[e^{-i(\mathbf{G}+\mathbf{q})\cdot\hat{\mathbf{r}}}, \hat{V}^{\mathrm{nl}}\right]|\delta\psi^\alpha_{n\mathbf{k},\mathbf{q}}\rangle \tag{71}$$

The first-order charge on the left-hand side of Eq. (69) can be obtained from a conventional DFPT phonon calculation, and thus Eq. (69) allows for several tests of our methodology.

A simple test of the nonlocal contribution at $\mathbf{q} = 0$ is to compare the dipole moment of the nonlocal charge with $\overline{P}^{\mathbf{q},\mathrm{nl}(0)}_{\alpha,\alpha}$ [i.e., the second term in Eq. (57)], which should give the nonlocal contribution to the Born effective charge

$$Z^*_{\alpha\beta,\mathrm{nl}} = \overline{P}^{\mathbf{q}=0,\mathrm{nl}}_{\alpha,\beta} = \int_{\mathrm{cell}} d^3 r \rho^{\mathrm{nl}}_{\beta\mathbf{q}=0}(\mathbf{r}) r_\alpha. \tag{72}$$

Again, this relation is generally applicable. For cubic symmetry, the Born effective charge tensor has only one independent element, which we write as $Z^* \equiv Z^{*\mathrm{NG}}_{\alpha\alpha}$. Of course, for the case of the noble gas atom "material," there is only one sublattice, so the sum of the nonlocal contribution with the local part (including the ionic charge) will vanish due to the acoustic sum rule (ASR).[63]

For the case of the isolated noble gas atoms, we can use Eqs. (68) and (69) to relate the real-space octupole moment of $\rho^{\mathrm{nl}}_{\alpha\mathbf{q}=0}(\mathbf{r})$ [Fourier transform of Eq. (71)] averaged over the cell, to the second $\mathbf{q}$ derivative of $\overline{P}^{\mathbf{q},\mathrm{nl}}_{\alpha,\alpha}$ [see Eq. (C1)] evaluated at $\mathbf{q} = 0$. Specifically, we should find that[15,17]

$$-\frac{1}{2}\frac{\partial^2 \overline{P}^{\mathbf{q},\mathrm{nl,NG}}_{\alpha,\alpha}}{\partial q_\alpha^2}\bigg|_{\mathbf{q}=0} = \frac{1}{6\Omega}\int_{\mathrm{cell}} d^3 r \rho^{\mathrm{nl,NG}}_{\alpha\mathbf{q}=0}(\mathbf{r}) r_\alpha^3, \tag{73}$$
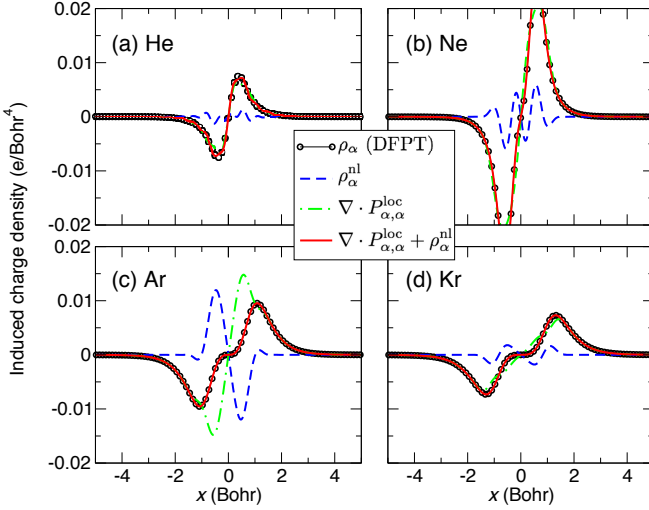
FIG. 1. (Color online) Planar average of the local [Eq. (70), green dot-dashed curve], nonlocal [Eq. (71), blue dashed], and total [Eq. (69), red solid] first-order charge for noble gas atoms displaced in the x direction by a $\mathbf{q} = 0$ phonon. The black circles correspond to the first-order charge calculated using a conventional, static, DFPT calculation. The box size is $16 \times 16 \times 16$ Bohr, but zoomed in to only show ± 5 Bohr.

and similarly for the local part,

$$
-\frac{1}{2} \frac{\partial^2 \overline{P}_{\alpha,\alpha}^{\mathbf{q},\mathrm{loc,NG}}}{\partial q_\alpha^2}\bigg|_{\mathbf{q}=0} = \frac{1}{6\Omega} \int_{\mathrm{cell}} d^3 r \left[-\nabla \cdot \mathbf{P}_{\alpha\mathbf{q}=0}^{\mathrm{loc,NG}}(\mathbf{r}) \right] r_\alpha^3,
\tag{74}
$$

where we again perform the reciprocal space calculations using mixed electrical boundary conditions.

The comparisons in Eqs. (73) and (74) test both the long-wavelength expansion of the current operator (local and nonlocal), and the accuracy of the adiabatic first-order wavefunction at finite $\mathbf{q}$.

4. Test of implementation: Longitudinal response

To test $P_{\alpha,\alpha\mathbf{q}=0}^{\mathrm{loc}}$ and $\delta\psi_{n\mathbf{k},\mathbf{q}=0}^{\alpha}$, we calculate the first-order charge [left-hand side of Eq. (69)] from a $\mathbf{q} = 0$ phonon by conventional DFPT, and compare to what we obtain for the right-hand side of Eq. (69) calculated using Eqs. (70) and (71) (with $\mathbf{q} = 0$). We Fourier transform the quantities in Eq. (69) to real space and plot their planar averages in Fig. 1 for for He, Ne, Ar, and Kr atoms in $16 \times 16 \times 16$ Bohr cells. Summing the contributions from the nonlocal charge (blue dashed curves) and the gradients of the local induced polarization (green dot-dashed) gives the red solid curves in Fig. 1. As expected from Eq. (69), the red curve lies on top of the black circles, which correspond to the first-order charge from the $\mathbf{q} = 0$ DFPT phonon calculations.

Now we can take the real-space moments of the curves in Fig. 1 and compare them with the results of our reciprocal space expansion. As discussed in the Sec. V A 3, the

TABLE II. Calculation of the Born effective charge and μ_{L} using the moments of the local and nonlocal charge (columns labeled ρ) compared to the current-density implementation (columns labelled P) for atoms in a $14 \times 14 \times 14$ Bohr box. Mixed electrical boundary conditions are used.

	Z^* (e)		μ_{L} (pC/m)			
	P^{nl}	ρ^{nl}	P^{loc}	ρ^{loc}	P^{nl}	ρ^{nl}
He	-0.027	-0.027	-0.470	-0.470	0.004	0.004
Ne	-0.155	-0.155	-1.872	-1.872	0.028	0.028
Ar	1.556	1.556	-4.620	-4.623	0.073	0.072
Kr	-0.214	-0.214	-5.878	-5.874	-0.099	-0.099

first moment of the blue dashed curves gives the nonlocal contribution to the Born effective charge, which should correspond to $\overline{P}_{\alpha,\alpha}^{\mathbf{q}=0,\mathrm{nl}}$ [Eq. (72)]. In Table II we give the nonlocal contribution to Z^* for the noble gas atoms in $14 \times 14 \times 14$ Bohr boxes. The ASR requires that the total Z^* vanishes; for our noble gas atoms, we calculate the magnitude of the total Z^* to be less than 10^{-4} e, so the "local" part (including the contribution from the ionic charge) is the same magnitude but opposite sign as the numbers in the second and third columns of Table II.

The second column of Table II, labeled P^{nl}, is calculated using the reciprocal space current and the third column (labeled ρ^{nl}) is from the real-space dipole moment of the charge density. We see that there is excellent agreement between the two methods, indicating that $\overline{P}_{\alpha,\alpha}^{\mathbf{q}=0,\mathrm{nl}}$ is accurately calculated.

It is also clear from Fig. 1 and Table II that the nonlocal correction to the Born effective charge can be very large, on the order of one electron for Ar. We see a similarly large contribution for atoms with empty $3d$ shells (but projectors in this channel) such as a Ca atom or Ti^{4+} ion (not shown).

Now we would like to test the accuracy of our long-wavelength expansion of the current operator (Sec. III C) for calculating μ_{L}. In Table II we give both the local and nonlocal contributions to μ_{L} using the right-hand side of Eqs. (73) and (74) (labeled as ρ^{loc} and ρ^{nl}), compared to those calculated from our current-density implementation [left-hand side of Eqs. (73) and (74), labeled as P^{loc} and P^{nl}]. The agreement between the real-space moments and reciprocal-space derivatives of the expansion in Eq. (57) is excellent. Also, we can see that even though the nonlocal contribution to the Born effective charge is large for Ar, the first-order nonlocal charge is almost purely dipolar, with the the third moment being almost two orders of magnitude smaller than the contribution of the local part.

Also, from Table III and Fig. 2, we see that $\mu_{\mathrm{L}} = Q_{\mathrm{NG}}/2\Omega$ [consistent with Eq. (67)] quite accurately for sufficiently large simulation cells.

TABLE III. Longitudinal and shear (ICL and PM path) FxE coefficients for noble gas atoms in $14 \times 14 \times 14$ Bohr boxes, as well as the diamagnetic susceptibility correction, χ_{mag} (ICL and PM path), and the quadrupole moment of the unperturbed charge density divided by two times the volume [*cf.* Eqs. (63) and (64)]. All quantities are in units of pC/m, and mixed electrical boundary conditions used.

	μ_{L}	$\mu_{\text{S}}^{\text{ICL}}$	$\mu_{\text{S}}^{\text{PM}}$	$\chi_{\text{mag}}^{\text{ICL}}$	$\chi_{\text{mag}}^{\text{PM}}$	$Q_{\text{NG}}/2\Omega$
He	-0.468	-0.467	-0.464	-0.468	-0.464	-0.466
Ne	-1.840	-1.693	-1.655	-1.692	-1.655	-1.845
Ar	-4.545	-5.008	-5.086	-5.013	-5.081	-4.554
Kr	-5.968	-5.901	-5.917	-5.903	-5.921	-5.990
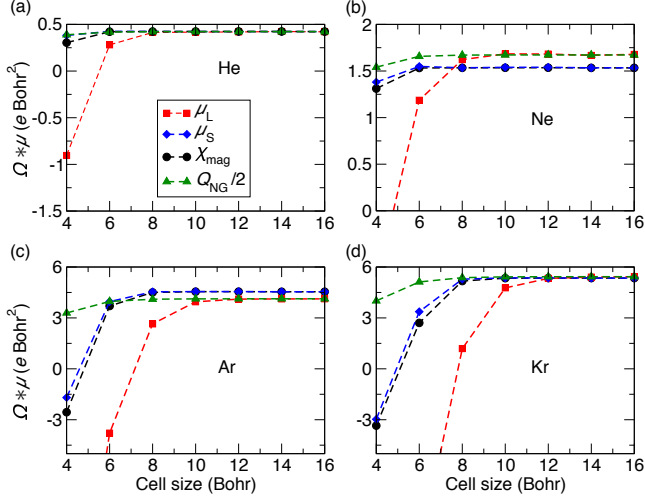
FIG. 2. (Color online) The longitudinal (red squares) and shear (blue diamonds) FxE coefficients, as well as the diamagnetic susceptibility correction (black circles) and $Q_{\text{NG}}/2\Omega$, for (a) He, (b) Ne, (c) Ar, and (d) Kr atoms in cells with various lattice constants. All quantities are multiplied by the cell volume, Ω.

5. *Test of implementation: Shear response*

In Table III we give the longitudinal and shear FxE coefficients, as well as χ_{mag} and $Q_{\text{NG}}/2\Omega$, for noble gas atoms in $14 \times 14 \times 14$ Bohr boxes. For μ_{S} and χ_{mag}, we give values using the ICL and PM paths for the nonlocal correction. In Fig. 2, we show the dependence of these quantities on the box size.

From Table III and Fig. 2, we see that $\mu_{\text{S}} = \chi_{\text{mag}}$ (consistent with the isotropic symmetry of the atoms) accurately for sufficiently large simulation cells. However, for atoms other than He, χ_{mag} is noticeably different from $Q_{\text{NG}}/2\Omega$, even for large box sizes. This discrepancy demonstrates that either Larmor's theorem or the Langevin theory of diamagnetism breaks down when nonlocal pseudopotentials are present (see Sec. VI for further discussion).

When we compare the two path choices, PM (Sec. III B 5) and ICL (Sec. III B 4), we find slight quan-titative differences for the shear component and diamagnetic correction. However, the differences between the paths vanishes for μ_{S}' [see Eq. (61)], indicating that although the CRG contribution is path-dependent, the "true" shear response (which is vanishing for spherical symmetry) is not for this system. This result is an excellent test that our implementation is sound. Indeed, for a cubic solid, all three components of the electronic flexoelectric tensor $\boldsymbol{\mu}'$ can be related to the surface charge accumulated via the mechanical deformation of a finite crystallite; thus, they shouldn't depend on the aforementioned path choice. As the path choice is irrelevant in our context, in the next Section we shall perform our calculations on cubic oxides using the ICL path. In Sec. VI we shall provide a critical discussion of the ICL and PM prescriptions from a more general perspective, and leave a detailed comparison of the two approaches for a future work.

B. Cubic oxides

We now apply our methodology to calculate the bulk, CI FxE coefficients for several technologically important cubic oxides. As mentioned before, we will be using short circuit boundary conditions and the ICL path for the nonlocal contribution.

As an example of a typical calculation, in Fig. 3 we plot the induced polarization [Eq. (57)] versus $\mathbf{q} = (q_x, 0, 0)$ for cubic $SrTiO_3$, both for polarization direction and atomic displacement $\alpha = \beta = x$ and $\alpha = \beta = y$. As expected, the dependence on q is quadratic (there is no linear term since cubic $SrTiO_3$ is not piezoelectric[15,17]), and $\overline{P}^{\mathbf{q}} = 0$ at $\mathbf{q} = 0$, which is required by the ASR condition that the sum of the Born effective charges should vanish.[63] By taking the second derivative of the black (red) dashed curves in Fig. 3, we can obtain $\mu_{11,11}^{\text{I}}$ ($\mu_{11,22}^{\text{I}}$). The remaining coefficient $\mu_{12,12}^{\text{I}}$ is obtained by calculating $\overline{P}_{12}^{\mathbf{q}}$ at various $\mathbf{q} = (q_x, q_y, 0)$, and performing a numerical mixed derivative $\partial^2/\partial q_x \partial q_y$ (not shown).

In Table IV, we give the FxE coefficients corrected for the CRG contribution [*cf.* Eq. (61)] and the RCC (Sec. IV C). As discussed above, the RCC is added to the longitudinal and transverse coefficients.[56] Note that the reported χ_{mag} is given in pC/m, whereas other quantities are in nC/m, so this correction is quite small for the materials calculated. The contribution of the nonlocal potentials to the FxE coefficients in Table IV, which are computed using the ICL path of Appendix C 1, represents a more significant correction than was the case in Sec. V A: they are in the range of 0.03 to 0.12 nC/m for the longitudinal and transverse coefficients, and in the range of -0.02 to 0.008 nC/m for the shear coefficients.

The only material for which first-principles calculations of the transverse and shear coefficients are available (in parentheses in Table IV) is $SrTiO_3$, and our values are in excellent agreement with those previous calculations.[19]

TABLE IV. Lattice constant, CI dielectric constant, rigid-core correction, and longitudinal, transverse, and shear CI FxE coefficients (under short circuit boundary conditions), as well as the diamagnetic susceptibility in units of nC/m. The FxE constants include the CRG correction (Sec. III D) and RCC (Sec. IV C).

	a (Bohr)	ϵ	RCC	μ'_L	μ'_T	μ'_S	$\chi_{\mathrm{mag}} \times 10^3$
$SrTiO_3$	7.435	6.191	-0.049	$-0.87\ (-0.9^a, -0.88^b)$	$-0.84\ (-0.83^b)$	$-0.08(-0.08^b)$	-7.3
$BaTiO_3$	7.601	6.657	-0.107	$-1.01\ (-1.1^a)$	-0.99	-0.08	-1.7
$SrZrO_3$	7.882	4.558	-0.049	-0.63	-0.58	-0.05	-36.0
$PbTiO_3$	7.496	8.370	-0.158	$-1.39\ (-1.5^a)$	-1.35	-0.09	-22.4
MgO	8.058	3.148	-0.015	$-0.28\ (-0.3^a)$	-0.30	-0.07	-66.1

[a] Ref. 17
[b] Ref. 19
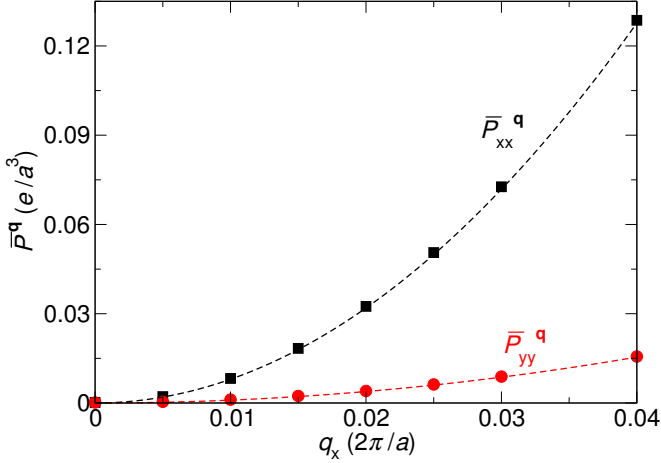
FIG. 3. (Color online) Induced polarization versus $\mathbf{q} = (q_x, 0, 0)$ for cubic $SrTiO_3$. The black (red) points correspond to the x (y) component of the polarization for atomic displacements of the atoms in the x (y) direction. Dashed curves are quadratic fits. Units are with respect to the calculated $SrTiO_3$ lattice constant $a = 7.435$ Bohr.

For all of the materials, the longitudinal and transverse responses are of similar magnitude, and the shear response is significantly smaller. This is a similar trend to that of the isolated noble gas atoms and of the IRC model [cf. Eq. (65)], suggesting that the response is dominated by the "spherical" contribution. The behavior of the cubic oxides differ significantly from the IRC model, however, when it comes to the contribution of the CRG correction χ_{mag}. For isolated atoms, χ_{mag} is equal to $\mu_{\mathrm{IRC},S}$, and is of the same order as $\mu'_{\mathrm{IRC},L}$; therefore, a vanishing value of $\mu'_{\mathrm{IRC},S}$ is only obtained after removing the CRG contribution [Eq. (61)]. In the case of the cubic oxides, the CRG correction is only a minor contribution to μ'_S, and χ_{mag} is two orders of magnitude smaller than μ'_L. In fact, χ_{mag} for the cubic oxides is comparable to that of the isolated atoms, while the FxE coefficients for the cubic oxides are two orders of magnitude larger. This indicates that although the bonding of atoms in the cubic compounds significantly enhances the FxE coefficients, it does not have a large effect on the CRG correction.

It should be noted that the value of χ_{mag} for $SrTiO_3$

(-2.28×10^{-7} cm^3/g after unit conversion) is in fair agreement with the measured diamagnetic susceptibility of around -1×10^{-7} cm^3/g from Ref. 64.

VI. DISCUSSION

Before closing, it is useful to recap the technical issues that are associated with the calculation of the current density response in a nonlocal pseudopotential context, and critically discuss them in light of the result presented in this work. In particular, it is important to clarify whether our proposed approach matches the expectations, especially regarding the known transformation properties of the current density upon rototranslations, or whether there is any deviation that needs to be kept in mind when computing flexoelectric coefficients and other current-related linear-response properties.

As we have already discussed at length in the earlier Sections, our definition of the current density (i) satisfies the continuity equation by construction, (ii) correctly reduces to the textbook formula in region of space where the Hamiltonian is local, and (iii) is consistent with the known formula for the macroscopic current operator. However, we have not yet discussed some additional properties of the current density that were established in earlier works, that might be used as "sanity checks" of our implementation:

- Translational invariance of the charge-density response: As established by Martin,[53] simultaneous uniform translation of all atoms in the crystal must yield the same variation in charge density at every point as if the static charge density were rigidly shifted. Therefore, if the whole crystal undergoes a translation with uniform velocity $\mathbf{v}$, the current density in the laboratory frame must be

$$\mathbf{J}(\mathbf{r}) = \mathbf{v}\rho(\mathbf{r}), \qquad (75)$$

where $\rho(\mathbf{r})$ is the static charge density.

- Larmor's theorem: The circulating currents generated in a crystallite by a uniform rotation with constant angular velocity $\boldsymbol{\omega}$ (as observed in the

frame of the rotating material) are, in the linear limit of small velocities, identical to the orbital currents that would be generated by an applied (and constant in time) **B**-field. As a corollary, the rotational g-factor of closed-shell molecules corresponds to their paramagnetic susceptibility.

- Langevin's diamagnetism: The magnetic susceptibility of a spherically symmetric atom is proportional to the quadrupolar moment of its ground-state charge density.

In the following, we shall analyze how our formalism stands in relationship to these latter "weak" [compared to the "strong" conditions (i-iii) above] criteria of validity. (By "weak" we mean not required for a physically sound calculation of the flexoelectric tensor, but possibly necessary for a wider range of physical properties.)

A. Translational invariance of the charge-density response

Based on our results of Table III, we can safely conclude that both flavors of the current-density operator (ICL and PM) break translational invariance, Eq. (75). To see this, consider the shear flexoelectric coefficient of an isolated atom in a box, (e.g., $\mu_{S,NG}$). This quantity can be defined in real space as the second moment of the microscopic current-density response to the displacement of an isolated atom,

$$\mu_S = \frac{1}{2\Omega} \int d^3 r \frac{\partial J_y(\mathbf{r})}{\partial \dot{\lambda}_y} x^2, \qquad (76)$$

where $\dot{\lambda}_y$ stands for the velocity of the atom along y. This formula, as it stands, is not very practical for calculations: our implementation does not allow for a fully microscopic calculation of $\mathbf{J}(\mathbf{r})$, and therefore we had to replace Eq. (76) with computationally more tractable small-$\mathbf{q}$ expansions. Still, Eq. (76) is quite useful for our purposes, as it allows us to draw general conclusions about $\mathbf{J}(\mathbf{r})$ without the need for calculating it explicitly. In particular, if translational invariance [Eq. (75)] were satisfied, then we could plug Eq. (75) into Eq. (76) and use Eq. (64) to obtain $\mu_{S,NG} = \frac{1}{2\Omega} \int d^3 r \rho(\mathbf{r}) x^2 = Q_{NG}/2\Omega$. [This equality is a necessary but not sufficient condition for the validity of Eq. (75).] As we can see from Table III, $\mu_{S,NG}$ is only approximately equal to $Q_{NG}/2\Omega$ for both the ICL and PM flavors of the current-density operator. This implies that neither approach is able to guarantee translational invariance.

Similarly, the data we have in hand does not allow us to establish a clear preference between the PM and ICL recipes, as the discrepancies between the two are typically much smaller (and devoid of a systematic trend) than their respective failure at satisfying $\mu_{S,NG} = Q_{NG}/2\Omega$. Note that the discrepancy strictly consists of *solenoidal*

(i.e., divergenceless) contributions to the current response; the longitudinal components are exactly treated, as one can verify from the excellent match between the longitudinal coefficient, μ_L, and the quadrupolar estimate in Table III.

B. Langevin diamagetism and Larmor's theorem

We come now to the assessment of the Larmor and Langevin results. One of the virtues of the PM recipe resides in its superior accuracy when comparing the orbital magnetic response to all-electron data. Indeed, in the context of our discussion, one can verify that it exactly complies with Langevin's theory of diamagnetism in the case of isolated spherical atoms.[65] The situation, however, is not so bright regarding Larmor's theorem. If the latter were satisfied, then the "rotational orbital susceptibility" χ_{mag} would match Langevin's quadrupolar expression, as we know that Langevin's result holds in the case of a "true" **B**-field. By looking, again, at Table III, we clearly see that this is not the case – again, there is a discrepancy between the last column (based on the static quadrupole) and the calculated values of χ_{mag}. Since the deviations in χ_{mag} and μ_S are essentially identical in the limit of an isolated atom in a box, it is reasonable to assume that the underlying factors are similar.

It should be noted that our value for Ne (after unit conversion, ICL path) is $\chi_{mag}^{ICL} = -7.29 \times 10^{-6}$ cm^3/mole, which is fairly close in magnitude to previously calculated values of the diamagnetic susceptibility of Ne: -7.75×10^{-6} cm^3/mole[33] and -7.79×10^{-6} cm^3/mole[35] (the sign is a matter of convention).

C. Unphysical spatial transfer resulting from nonlocal pseudopotentials

The reason why the current density violates both translational invariance and Larmor's theorem has to be sought in the unphysical transfer of density that can result from the presence of a nonlocal potential. That is, a nonlocal operator may project the wavefunction (and therefore the particle amplitude) from a point $\mathbf{r}$ to a distant point $\mathbf{r}'$ in a discontinuous manner, such that no current flows through a given surface surrounding $\mathbf{r}$ even though the charge density within that surface changes. Of course, this is just a conceptual way of describing the violation of the continuity equation, discussed in Sec. III B.

Taking the example of a single atom placed at $\mathbf{R} = 0$ and using the PM approach, it is shown in Appendix E that the current density can be written as

$$\mathbf{J}^{nl}(\mathbf{r}) \sim \frac{\hat{\mathbf{r}} C(\hat{\mathbf{r}})}{r^2}. \qquad (77)$$

where $C(\hat{\mathbf{r}})$ is a direction-dependent constant that depends on the nonlocal charge [Eq. (E5)]. Therefore, the current-density field diverges near the atomic site, $\mathbf{r} \to 0$, and such a divergence can have a different prefactor and sign depending on the direction.

A diverging $\mathbf{J}$-field is problematic to deal with and unphysical. One can easily realize that this characteristic is incompatible, for example, with the correct transformation laws of $\mathbf{J}$ under rigid translations. In particular, the electronic charge density is always finite in a vicinity of the nucleus, even in the all-electron case where the corresponding potential does, in fact, diverge. This implies that Eq. (75) cannot be satisfied by a diverging $\mathbf{J}$-field.

For the ICL path, the nonlocal current does not have such a simple relation to the nonlocal charge as in the case of the PM path [Eq. (E4)]; therefore a similar derivation as in Appendix E may not be possible for the ICL case. However, our numerical results in Table III are sufficient to conclude that the ICL path violates translational symmetry as well. The extent of the violation can be quantified by looking at the discrepancy between μ_L and μ_S, which is comparably large in the PM and ICL cases—recall that these two values should, in principle, coincide for the isolated spherical atoms model.

At present it is difficult to predict whether it might be possible to cure the above drawbacks by simply choosing a different path for the definition of the current operator, or whether these difficulties may require a deeper revision of the nonlocal pseudopotential theory in contexts where the microscopic current density is needed. In any case, the flexoelectric coefficients we calculated in this work for cubic materials are unaffected by these issues: Once the "diamagnetic" contribution has been removed, the three independent coefficients are all well defined in terms of the charge-density response. Nonetheless, the above caveats should be kept in mind when using the present current-density implementation to access flexoelectric coefficients in less symmetric materials, or other response properties that depend on the microscopic current response.

VII. CONCLUSIONS

We have developed a DFPT implementation for calculating the bulk CI flexoelectric tensor from a single unit cell. Therefore, we have overcome the limitations of previous implementations (Refs. 17 and 19), which required supercells to calculate the transverse and shear CI FxE coefficients.

Our implementation is based on calculating the microscopic current density resulting from the adiabatic atomic displacements of a long-wavelength acoustic phonon. We have determined a form for the current-density operator that satisfies the continuity condition in the presence of nonlocal, norm-conserving pseudopotentials, and reduces to the correct form in the limit of a uniform, macroscopic perturbation, and/or when only local potentials are present.

In order to benchmark our methodology, we have used noble gas atoms to model systems of noninteracting spherical charge densities. The tests demonstrate the accuracy of our nonlocal correction to the current operator, as well as the calculated CRG corrections derived in Ref. 24. For our form of the current density, we demonstrate that nonlocal pseudopotentials result in a violation of translational invariance and Larmor's theorem, though this does not affect our FxE coefficients after the CRG contribution has been removed. Finally, we have applied our methodology to several cubic oxides, all of which show similar trends in that the longitudinal and transverse responses are similar (~ 1 nC/m), and the shear response is an order of magnitude smaller.

Combining the methodology of this paper with DFPT implementations for calculating the lattice-mediated contribution to the bulk FxE coefficients,[15,19] and the surface contribution,[19] will allow for efficient calculation of the full FxE response for a variety of materials.

Appendix A: Essin *et al.* approach and the Ismail-Beigi, Chang, and Louie straight-line path

Here we perform a long-wavelength expansion of the current operator using the approach of Essin *et al.*,[51] and confirm that the approach is equivalent to that of ICL.[33] We start from Eq. (45) and rewrite it as

$$
\begin{aligned}
\langle \mathbf{s} | \hat{\mathcal{J}}_\alpha^{\text{ICL}}(\mathbf{q}) | \mathbf{s}' \rangle &= -i H(\mathbf{s}, \mathbf{s}')(s_\alpha - s'_\alpha) \frac{e^{-i\mathbf{q}\cdot\mathbf{s}} - e^{-i\mathbf{q}\cdot\mathbf{s}'}}{i\mathbf{q}\cdot(\mathbf{s}-\mathbf{s}')} \\
&= -i \left[\hat{r}_\alpha, \hat{H} \right]_{\mathbf{s}\mathbf{s}'} \frac{e^{-i\mathbf{q}\cdot\mathbf{s}} - e^{-i\mathbf{q}\cdot\mathbf{s}'}}{i\mathbf{q}\cdot(\mathbf{s}-\mathbf{s}')} \\
&= - \left(i \left[\hat{r}_\alpha, \hat{T} \right]_{\mathbf{s}\mathbf{s}'} + i \left[\hat{r}_\alpha, \hat{V}^{\text{nl}} \right]_{\mathbf{s}\mathbf{s}'} \right) \frac{e^{-i\mathbf{q}\cdot\mathbf{s}} - e^{-i\mathbf{q}\cdot\mathbf{s}'}}{i\mathbf{q}\cdot(\mathbf{s}-\mathbf{s}')},
\end{aligned}
\tag{A1}
$$

where $\hat{T}$ is the kinetic energy operator and $\hat{V}^{\text{nl}}$ is the nonlocal part of the potential (the local part of the potential does not contribute). We now factor out a $e^{-i\mathbf{q}\cdot\mathbf{s}'}$ and then expand the term outside of the parentheses

$$
\langle \mathbf{s} | \hat{\mathcal{J}}_\alpha^{\text{ICL}}(\mathbf{q}) | \mathbf{s}' \rangle = - \left(i \left[\hat{r}_\alpha, \hat{T} \right]_{\mathbf{s}\mathbf{s}'} + i \left[\hat{r}_\alpha, \hat{V}^{\text{nl}} \right]_{\mathbf{s}\mathbf{s}'} \right) e^{-i\mathbf{q}\cdot\mathbf{s}'} \left(-1 + \frac{i\mathbf{q}\cdot(\mathbf{s}-\mathbf{s}')}{2} + \frac{[\mathbf{q}\cdot(\mathbf{s}-\mathbf{s}')]^2}{6} + ... \right).
\tag{A2}
$$

As mentioned in Sec. III B 4, if $\mathbf{q} = 0$, then $\hat{\mathcal{J}}_\alpha^{\text{ICL}}(\mathbf{q} = 0) = i \left[\hat{r}_\alpha, \hat{H} \right] = -\hat{v}_\alpha$, the velocity operator.

Consider the case of a Hamiltonian with a local potential, so the only term in Eq. (A2) is the commutator of the position operator with the kinetic part of the Hamiltonian. We can rewrite this term as

$$
\langle \mathbf{s} | \hat{\mathcal{J}}_\alpha^{\text{loc}}(\mathbf{q}) | \mathbf{s}' \rangle = - \left(-i \left[\hat{r}_\alpha, \hat{T} \right]_{\mathbf{s}\mathbf{s}'} - \sum_{\gamma=1}^3 \frac{q_\gamma}{2} \left[\hat{r}_\gamma, \left[\hat{r}_\alpha, \hat{T} \right] \right]_{\mathbf{s}\mathbf{s}'} + \sum_{\gamma=1}^3 \sum_{\xi=1}^3 \frac{i q_\gamma q_\xi}{6} \left[\hat{r}_\xi, \left[\hat{r}_\gamma, \left[\hat{r}_\alpha, \hat{T} \right] \right] \right]_{\mathbf{s}\mathbf{s}'} + ... \right) e^{-i\mathbf{q}\cdot\mathbf{s}'}.
\tag{A3}
$$

The term at zeroth order in q is simply the momentum operator: $\hat{p}_\alpha = -i \left[\hat{r}_\alpha, \hat{T} \right]$; at first order in q, we have $\hat{q}_\alpha/2$ (the nested commutator is simply the Kroneker delta function $-\delta_{\alpha\gamma}$); higher order terms vanish. So in the case of a Hamiltonian that only has a local potential,

$$
\hat{\mathcal{J}}_\alpha^{\mathbf{q},\text{loc}} = - \left(\hat{p}_\alpha + \frac{q_\alpha}{2} \right),
\tag{A4}
$$

which is the cell-periodic momentum operator for the case of local potentials, as we derive in Appendix B. Therefore the local and nonlocal components can be cleanly separated. The nonlocal part of the potential in Eq. A1 is addressed in Appendix C 1.

Note that the approach of Essin *et al.* does not work for an arbitrary choice of path. Specifically, if we were to use Eq. (42) with the PM path choice $\mathbf{s}' \to \mathbf{R} \to \mathbf{s}$, the expression would not reproduce the correct form of the current for local potentials (except for the case of the longitudinal response). Of course, in the PM form of the coupled Hamiltonian in Eq. (48), the current in the case of only local potentials trivially reduces to the correct form $\hat{\mathcal{J}}_\alpha^{\text{loc}}(\mathbf{r}) = -\frac{1}{2} \left\{ \hat{\rho}(\mathbf{r}), (\hat{p}_\alpha + \hat{A}_\alpha) \right\}$.

Appendix B: Derivation of induced polarization: Local potentials

In this section we derive $P_{\alpha,\kappa\beta}^{\mathbf{q},\text{loc}}$ for Eq. (54). This is a straightforward generalization of what was derived by Umari, Dal Corso, and Resta[31] to finite $\mathbf{q}$ perturbations, and has been derived previously in other contexts (e.g. for determining magnetic[35] or dielectric[45] susceptibility, and in the context of phonon deformation potentials[66]).

Using the adiabatic expansion of the time-dependent wavefunction [Eqs. (10) and (11)], to first order in $\dot{\lambda}$ we can write the density matrix as

$$
\rho(t) = -\frac{2}{N_k} \sum_{n\mathbf{k}} |\Psi_{n\mathbf{k}}(\lambda(t))\rangle \langle \Psi_{n\mathbf{k}}(\lambda(t))| \simeq -\frac{2}{N_k} \sum_{n\mathbf{k}} \left[|\psi_{n\mathbf{k}}\rangle\langle\psi_{n\mathbf{k}}| + \dot{\lambda}(|\delta\psi_{n\mathbf{k}}\rangle\langle\psi_{n\mathbf{k}}| + |\psi_{n\mathbf{k}}\rangle\langle\delta\psi_{n\mathbf{k}}|) \right]
\tag{B1}
$$

where the factor of two is assuming spin degeneracy. If we apply the local current-density operator [Eq. (29)], retaining terms only to linear order in $\dot{\lambda}$, and take the derivative with respect to $\dot{\lambda}$ we obtain the induced polarization

$$
P_\alpha^{\text{loc}}(\mathbf{r}) = -\frac{1}{N_k} \sum_{n\mathbf{k}} \left[\langle\psi_{n\mathbf{k}}|\mathbf{r}\rangle\langle\mathbf{r}|\hat{p}_\alpha|\delta\psi_{n\mathbf{k}}\rangle + \langle\delta\psi_{n\mathbf{k}}|\mathbf{r}\rangle\langle\mathbf{r}|\hat{p}_\alpha|\psi_{n\mathbf{k}}\rangle + \langle\psi_{n\mathbf{k}}|\hat{p}_\alpha|\mathbf{r}\rangle\langle\mathbf{r}|\delta\psi_{n\mathbf{k}}\rangle + \langle\delta\psi_{n\mathbf{k}}|\hat{p}_\alpha|\mathbf{r}\rangle\langle\mathbf{r}|\psi_{n\mathbf{k}}\rangle \right].
\tag{B2}
$$

Now consider the perturbation in Eq. (3): the displacement of a sublattice κ in direction β modulated by a phase with wavevector $\mathbf{q}$. We begin with the real-space expression for the polarization induced by this perturbation:

$$P_{\alpha,\kappa\beta}^{\mathbf{q},\mathrm{loc}}(\mathbf{r}) = -\frac{1}{N_k}\sum_{n\mathbf{k}}\left[\langle\psi_{n\mathbf{k}}|\mathbf{r}\rangle\langle\mathbf{r}|\hat{p}_\alpha|\delta\psi_{n\mathbf{k},\mathbf{q}}^{\kappa\beta}\rangle + \langle\delta\psi_{n\mathbf{k},-\mathbf{q}}^{\kappa\beta}|\mathbf{r}\rangle\langle\mathbf{r}|\hat{p}_\alpha|\psi_{n\mathbf{k}}\rangle + \langle\psi_{n\mathbf{k}}|\hat{p}_\alpha|\mathbf{r}\rangle\langle\mathbf{r}|\delta\psi_{n\mathbf{k},\mathbf{q}}^{\kappa\beta}\rangle + \langle\delta\psi_{n\mathbf{k},-\mathbf{q}}^{\kappa\beta}|\hat{p}_\alpha|\mathbf{r}\rangle\langle\mathbf{r}|\psi_{n\mathbf{k}}\rangle\right]$$

(B3)

where the subscript $\mathbf{q}$ in $\delta\psi_{n\mathbf{k},\pm\mathbf{q}}^{\kappa\beta}$ indicates that the perturbation couples states at $\mathbf{k}$ to those at $\mathbf{k}\pm\mathbf{q}$. If we assume TRS [see Eq. (24)], then we have

$$P_{\alpha,\kappa\beta}^{\mathbf{q},\mathrm{loc}}(\mathbf{r}) = -\frac{2}{N_k}\sum_{n\mathbf{k}}\left[\langle\psi_{n\mathbf{k}}|\mathbf{r}\rangle\langle\mathbf{r}|\hat{p}_\alpha|\delta\psi_{n\mathbf{k},\mathbf{q}}^{\kappa\beta}\rangle + \langle\psi_{n\mathbf{k}}|\hat{p}_\alpha|\mathbf{r}\rangle\langle\mathbf{r}|\delta\psi_{n\mathbf{k},\mathbf{q}}^{\kappa\beta}\rangle\right]$$

(B4)

We Fourier transform Eq. (B4) to reciprocal space and consider the cell periodic part

$$P_{\alpha,\kappa\beta}^{\mathrm{loc}}(\mathbf{G}+\mathbf{q}) = -\frac{2}{N_k}\sum_{n\mathbf{k}}\int d^3r\left[\langle\psi_{n\mathbf{k}}|\mathbf{r}\rangle e^{-i(\mathbf{G}+\mathbf{q})\cdot\mathbf{r}}\langle\mathbf{r}|\hat{p}_\alpha|\delta\psi_{n\mathbf{k},\mathbf{q}}^{\kappa\beta}\rangle + \langle\psi_{n\mathbf{k}}|\hat{p}_\alpha|\mathbf{r}\rangle e^{-i(\mathbf{G}+\mathbf{q})\cdot\mathbf{r}}\langle\mathbf{r}|\delta\psi_{n\mathbf{k},\mathbf{q}}^{\kappa\beta}\rangle\right].$$

(B5)

We now explicitly insert the expansion of the wavefunctions in terms of plane waves

$$\psi_{\mathbf{k}}(\mathbf{s}) = \sum_m c_{\mathbf{k},\mathbf{G}_m}e^{i(\mathbf{G}_m+\mathbf{k})\cdot\mathbf{s}}$$

$$\delta\psi_{n\mathbf{k},\mathbf{q}}^{\kappa\beta}(\mathbf{s}) = \sum_m \delta c_{\mathbf{k}+\mathbf{q},\mathbf{G}_m}e^{i(\mathbf{G}_m+\mathbf{k}+\mathbf{q})\cdot\mathbf{s}},$$

(B6)

where we have dropped the band index and the $\kappa\beta$ indices for the expansion coefficients c and δc, and m indexes a reciprocal lattice vector $\mathbf{G}_m$. Then, applying the momentum operator,

$$P_{\alpha,\kappa\beta}^{\mathrm{loc}}(\mathbf{G}+\mathbf{q}) = -\frac{2}{N_k}\sum_{\mathbf{k}}\sum_{m,m'}\int d^3r c_{\mathbf{k},\mathbf{G}_m}^* \delta c_{\mathbf{k}+q_\alpha,\mathbf{G}_{m'}}\left[(k_\alpha+q_\alpha+G_{\alpha,m'})e^{-i(\mathbf{G}+\mathbf{G}_m-\mathbf{G}_{m'})\cdot\mathbf{r}}\right.$$

$$\left. + (k_\alpha+G_{\alpha,m})e^{-i(\mathbf{G}+\mathbf{G}_m-\mathbf{G}_{m'})\cdot\mathbf{r}}\right]$$

$$= -\frac{4}{N_k}\sum_{\mathbf{k}}\sum_m c_{\mathbf{k},\mathbf{G}_m}^* \delta c_{\mathbf{k}+q_\alpha,\mathbf{G}_m+\mathbf{G}}\left(k_\alpha+G_{\alpha,m}+\frac{q_\alpha+G_\alpha}{2}\right)$$

$$= -\frac{2}{N_k}\sum_{n\mathbf{k}}\langle u_{n\mathbf{k}}|e^{-i\mathbf{G}\cdot\hat{\mathbf{r}}}\left(\hat{p}_\alpha^{\mathbf{k}}+\frac{q_\alpha}{2}\right) + \left(\hat{p}_\alpha^{\mathbf{k}}+\frac{q_\alpha}{2}\right)e^{-i\mathbf{G}\cdot\hat{\mathbf{r}}}|\delta u_{n\mathbf{k},\mathbf{q}}^{\kappa\beta}\rangle,$$

(B7)

where, in the last line, we have restored the band and $\kappa\beta$ indices, $\hat{p}_\alpha^{\mathbf{k}} = -i\hat{\nabla}_\alpha + k_\alpha$ is the cell-periodic momentum operator ($\hat{\nabla}_\alpha$ is a spatial derivative in the α direction), and we have used that $\psi_{n\mathbf{k}}(\mathbf{s}) = u_{n\mathbf{k}}(\mathbf{s})e^{i\mathbf{k}\cdot\mathbf{s}}$. In Sec. V A, we use this result to calculate real-space moments of the local contribution to the FxE coefficient. Otherwise, we are usually interested in the $\mathbf{G} = 0$ term:

$$\overline{P}_{\alpha,\kappa\beta}^{\mathbf{q},\mathrm{loc}} = -\frac{4}{N_k}\sum_{n\mathbf{k}}\langle u_{n\mathbf{k}}|\left(\hat{p}_\alpha^{\mathbf{k}}+\frac{q_\alpha}{2}\right)|\delta u_{n\mathbf{k},\mathbf{q}}^{\kappa\beta}\rangle.$$

(B8)

Appendix C: Current density in the presence of nonlocal pseudopotentials

Here we derive the contributions to the current from the nonlocal potentials [$P_{\alpha,\kappa\beta}^{\mathbf{q},\mathrm{nl}}$ in Eq. (54)], which we obtain by expanding the nonlocal current-density operator up to second order in $\mathbf{q}$ [Eq. (53)],

$$\overline{P}_{\alpha,\kappa\beta}^{\mathbf{q},\mathrm{nl}} \simeq \frac{4}{N_k}\sum_{n\mathbf{k}}\left[\langle u_{n\mathbf{k}}|\hat{\mathcal{J}}_\alpha^{\mathbf{k},\mathrm{nl}(0)}|\delta u_{n\mathbf{k},\mathbf{q}}^{\kappa\beta}\rangle + \frac{1}{2}\sum_{\gamma=1}^3 q_\gamma\langle u_{n\mathbf{k}}|\hat{\mathcal{J}}_{\alpha,\gamma}^{\mathbf{k},\mathrm{nl}(1)}|\delta u_{n\mathbf{k},\mathbf{q}}^{\kappa\beta}\rangle + \frac{1}{6}\sum_{\gamma=1}^3\sum_{\xi=1}^3 q_\gamma q_\xi\langle u_{n\mathbf{k}}|\hat{\mathcal{J}}_{\alpha,\gamma\xi}^{\mathbf{k},\mathrm{nl}(2)}|\delta u_{n\mathbf{k},\mathbf{q}}^{\kappa\beta}\rangle\right], \quad (C1)$$

The nonlocal potential that we are interested in is that of the norm-conserving pseudopotential. In reciprocal space, the nonlocal potential in the separable Kleinman-Bylander[29] form is given by[67]

$$V^{\mathrm{nl}}(\mathbf{K},\mathbf{K}') = \sum_\zeta e^{-i\mathbf{K}\cdot\mathbf{R}_\zeta}\left(\sum_{lm}\frac{Y_{\zeta lm}^*(\hat{\mathbf{K}})T_{\zeta l}^*(|\mathbf{K}|)\times T_{\zeta l}(|\mathbf{K}'|)Y_{\zeta lm}(\hat{\mathbf{K}}')}{E_{\zeta l}^{\mathrm{KB}}}\right)e^{i\mathbf{K}'\cdot\mathbf{R}_\zeta}$$

(C2)

where $\mathbf{K} = \mathbf{G} + \mathbf{k}$; $\mathbf{R}_\zeta$ is the atomic position of atom ζ; $Y_{\zeta lm}$ is the spherical harmonic for the lm angular momentum channel; $T_{\zeta l}(K)$ is the Fourier transform of the radial function, $\widetilde{\psi}_{\zeta l}(r)V_{\zeta l}(r)$, where $V_{\zeta l}(r)$ are the pseudopotentials and $\widetilde{\psi}_{\zeta l}(r)$ the pseudoorbitals; $E^{\mathrm{KB}}_{\zeta l} = \langle \widetilde{\psi}_{\zeta l}|\hat{V}_l|\widetilde{\psi}_{\zeta l}\rangle$ is the Kleinman-Bylander energies. The term in the parentheses is the nonlocal form factor, and the phase factors surrounding it are the structure factors. We define

$$\langle \mathbf{K}|\phi_{\zeta lm}\rangle = e^{i\mathbf{K}\cdot\mathbf{R}_\zeta}Y_{\zeta lm}(\hat{\mathbf{K}})T_{\zeta l}(|\mathbf{K}|) \tag{C3}$$

so

$$\hat{V}^{\mathrm{nl}} = \sum_{\zeta lm} \frac{|\phi_{\zeta lm}\rangle\langle\phi_{\zeta lm}|}{E^{\mathrm{KB}}_{\zeta l}}. \tag{C4}$$

1. Ismail-Beigi, Chang, and Louie straight-line path

For the straight-line path of Essin *et al.*[51] and Ismail-Beigi, Chang, and Louie,[33] we combine Eq. (46) and (assuming we have TRS) Eq. (25). Since we have already addressed the local part in Appendix B, we only consider the nonlocal part of the Hamiltonian, defining the operator

$$\langle\mathbf{s}|\hat{\mathcal{J}}^{\mathbf{k},\mathbf{q},\mathrm{ICL},\mathrm{nl}}_\alpha|\mathbf{s}'\rangle = -iV^{\mathbf{k},\mathrm{nl}}(\mathbf{s},\mathbf{s}')(s_\alpha - s'_\alpha)\left[\frac{e^{-i\mathbf{q}\cdot(\mathbf{s}-\mathbf{s}')} - 1}{i\mathbf{q}\cdot(\mathbf{s}-\mathbf{s}')}\right]. \tag{C5}$$

Expanding the term in square brackets in powers of $\mathbf{q}$ gives

$$\langle\mathbf{s}|\hat{\mathcal{J}}^{\mathbf{k},\mathbf{q},\mathrm{ICL},\mathrm{nl}}_\alpha|\mathbf{s}'\rangle = iV^{\mathbf{k},\mathrm{nl}}(\mathbf{s},\mathbf{s}')(s_\alpha - s'_\alpha)\left[1 - \frac{i\mathbf{q}\cdot(\mathbf{s}-\mathbf{s}')}{2} + \frac{[i\mathbf{q}\cdot(\mathbf{s}-\mathbf{s}')]^2}{6} - \cdots\right].$$

$$= i\left[\hat{r}_\alpha, \hat{V}^{\mathbf{k},\mathrm{nl}}\right]_{\mathbf{ss}'} - \frac{1}{2}\sum_{\gamma=1}^{3}q_\gamma\left[\hat{r}_\gamma, \left[\hat{r}_\alpha, \hat{V}^{\mathbf{k},\mathrm{nl}}\right]\right]_{\mathbf{ss}'} - \frac{i}{6}\sum_{\gamma=1}^{3}\sum_{\xi=1}^{3}q_\gamma q_\xi\left[\hat{r}_\xi, \left[\hat{r}_\gamma, \left[\hat{r}_\alpha, \hat{V}^{\mathbf{k},\mathrm{nl}}\right]\right]\right]_{\mathbf{ss}'} + \cdots, \tag{C6}$$

so we can write the operator as

$$\hat{\mathcal{J}}^{\mathbf{k},\mathbf{q},\mathrm{ICL},\mathrm{nl}}_\alpha = \sum_{\gamma_1\cdots\gamma_n}\frac{q_{\gamma_1}\cdots q_{\gamma_n}}{(n+1)!}\hat{\mathcal{J}}^{\mathbf{k},\mathrm{ICL},\mathrm{nl}(n)}_{\alpha,\gamma_1\cdots\gamma_n}, \qquad \hat{\mathcal{J}}^{\mathbf{k},\mathrm{ICL},\mathrm{nl}(n)}_{\alpha,\gamma_1\cdots\gamma_n} = -\frac{\partial^{n+1}\hat{V}^{\mathbf{k},\mathrm{nl}}}{\partial k_\alpha\partial k_{\gamma_1}\cdots\partial k_{\gamma_n}}. \tag{C7}$$

In terms of the cell-periodic projectors $\phi^{\mathbf{k}}_{\zeta lm}(\mathbf{s}) = e^{-i\mathbf{k}\cdot\mathbf{s}}\phi_{\zeta lm}(\mathbf{s})$ [see Eq. (C4)], the lowest-order terms in Eq. (C7), to be incorporated into Eq. (C1), are

$$\hat{\mathcal{J}}^{\mathbf{k},\mathrm{nl}(0)}_\alpha = -\sum_{\zeta lm}\frac{1}{E^{\mathrm{KB}}_{\zeta l}}\left(|\phi^{\mathbf{k}}_{\zeta lm}\rangle\langle\partial_\alpha\phi^{\mathbf{k}}_{\zeta lm}| + |\partial_\alpha\phi^{\mathbf{k}}_{\zeta lm}\rangle\langle\phi^{\mathbf{k}}_{\zeta lm}|\right), \tag{C8}$$

$$\hat{\mathcal{J}}^{\mathbf{k},\mathrm{ICL},\mathrm{nl}(1)}_{\alpha,\gamma} = -\sum_{\zeta lm}\frac{1}{E^{\mathrm{KB}}_{\zeta l}}\left(|\partial_\gamma\phi^{\mathbf{k}}_{\zeta lm}\rangle\langle\partial_\alpha\phi^{\mathbf{k}}_{\zeta lm}| + |\phi^{\mathbf{k}}_{\zeta lm}\rangle\langle\partial_\alpha\partial_\gamma\phi^{\mathbf{k}}_{\zeta lm}| + |\partial_\alpha\partial_\gamma\phi^{\mathbf{k}}_{\zeta lm}\rangle\langle\phi^{\mathbf{k}}_{\zeta lm}| + |\partial_\alpha\phi^{\mathbf{k}}_{\zeta lm}\rangle\langle\partial_\gamma\phi^{\mathbf{k}}_{\zeta lm}|\right), \tag{C9}$$

and

$$\hat{\mathcal{J}}^{\mathbf{k},\mathrm{ICL},\mathrm{nl}(2)}_{\alpha,\gamma\xi} = -\sum_{\zeta lm}\frac{1}{E^{\mathrm{KB}}_{\zeta l}}\big(|\partial_\xi\partial_\gamma\phi^{\mathbf{k}}_{\zeta lm}\rangle\langle\partial_\alpha\phi^{\mathbf{k}}_{\zeta lm}| + |\partial_\xi\phi^{\mathbf{k}}_{\zeta lm}\rangle\langle\partial_\gamma\partial_\alpha\phi^{\mathbf{k}}_{\zeta lm}| + |\partial_\gamma\phi^{\mathbf{k}}_{\zeta lm}\rangle\langle\partial_\alpha\partial_\xi\phi^{\mathbf{k}}_{\zeta lm}| + \langle u_{n\mathbf{k}}|\phi^{\mathbf{k}}_{\zeta lm}\rangle\langle\partial_\gamma\partial_\alpha\partial_\xi\phi^{\mathbf{k}}_{\zeta lm}|$$

$$+ |\partial_\gamma\partial_\alpha\partial_\xi\phi^{\mathbf{k}}_{\zeta lm}\rangle\langle\phi^{\mathbf{k}}_{\zeta lm}| + \langle u_{n\mathbf{k}}|\partial_\alpha\partial_\xi\phi^{\mathbf{k}}_{\zeta lm}\rangle\langle\partial_\gamma\phi^{\mathbf{k}}_{\zeta lm}| + |\partial_\gamma\partial_\alpha\phi^{\mathbf{k}}_{\zeta lm}\rangle\langle\partial_\xi\phi^{\mathbf{k}}_{\zeta lm}| + |\partial_\alpha\phi^{\mathbf{k}}_{\zeta lm}\rangle\langle\partial_\gamma\partial_\xi\phi^{\mathbf{k}}_{\zeta lm}|\big). \tag{C10}$$

These correspond to last three terms in Eq. (53), here specialized to the ICL path. Note that $\hat{\mathcal{J}}^{\mathbf{k},\mathrm{nl}(0)}_\alpha = -\partial\hat{V}^{\mathbf{k},\mathrm{nl}}/\partial k_\alpha$ represents the well-known nonlocal correction to the Born effective charge (with an overall negative sign from the electron charge), which, combined with the local part [Eq. (B8)] yields the velocity operator $\hat{v}^{\mathbf{k},\mathbf{q}}_\alpha$ and should be unsensitive to the path choice.

2. Pickard and Mauri path through atom center

The PM[34] path goes through the center of the atom. For simplicity of the derivation, we consider a single atom positioned at the origin ($\mathbf{R} = 0$); the generalization to an atom not at the origin simply involves an extra phase in the structure factors in Eq. (C2). Then Eq. (51) becomes

$$\langle \mathbf{s} | \hat{\mathcal{J}}_\alpha^{\mathrm{PM,nl}}(\mathbf{q}) | \mathbf{s}' \rangle = -i V^{\mathrm{nl}}(\mathbf{s}, \mathbf{s}') \left[s_\alpha' \frac{1 - e^{-i\mathbf{q}\cdot\mathbf{s}'}}{i\mathbf{q}\cdot\mathbf{s}'} + s_\alpha \frac{e^{-i\mathbf{q}\cdot\mathbf{s}} - 1}{i\mathbf{q}\cdot\mathbf{s}} \right]. \tag{C11}$$

Following the same steps as in Appendix C 1, we arrive at slightly different current operators for the terms to first and second order in $\mathbf{q}$ (the zeroth order term is the same as for the ICL path, as expected),

$$\hat{\mathcal{J}}_{\alpha,\gamma}^{\mathbf{k},\mathrm{PM,nl}(1)} = -\sum_{\zeta l m} \frac{1}{E_{\zeta l}^{\mathrm{KB}}} \left(2|\partial_\alpha \phi_{\zeta l m}^{\mathbf{k}}\rangle\langle\partial_\gamma \phi_{\zeta l m}^{\mathbf{k}}| + |\phi_{\zeta l m}^{\mathbf{k}}\rangle\langle\partial_\alpha\partial_\gamma \phi_{\zeta l m}^{\mathbf{k}}| + |\partial_\alpha\partial_\gamma \phi_{\zeta l m}^{\mathbf{k}}\rangle\langle\phi_{\zeta l m}^{\mathbf{k}}| \right), \tag{C12}$$

$$\hat{\mathcal{J}}_{\alpha,\gamma\xi}^{\mathbf{k},\mathrm{PM,nl}(2)} = -\sum_{\zeta l m} \frac{1}{E_{\zeta l}^{\mathrm{KB}}} \left(3|\partial_\alpha\partial_\gamma \phi_{\zeta l m}^{\mathbf{k}}\rangle\langle\partial_\xi \phi_{\zeta l m}^{\mathbf{k}}| + 3|\partial_\alpha \phi_{\zeta l m}^{\mathbf{k}}\rangle\langle\partial_\gamma\partial_\xi \phi_{\zeta l m}^{\mathbf{k}}| + |\phi_{\zeta l m}^{\mathbf{k}}\rangle\langle\partial_\alpha\partial_\gamma\partial_\xi \phi_{\zeta l m}^{\mathbf{k}}| + |\partial_\alpha\partial_\gamma\partial_\xi \phi_{\zeta l m}^{\mathbf{k}}\rangle\langle\phi_{\zeta l m}^{\mathbf{k}}| \right). \tag{C13}$$

We see immediately that, for the case of a longitudinal perturbation, Eqs. (C12) and (C13) are identical to their ICL counterparts [cf. Eq. (C9) and Eq. (C10)].

Appendix D: Diamagnetic correction

In this section we provide some details about the calculation of the CRG contribution to the transverse and shear FxE coefficients, which is related to the diamagnetic susceptibility. We refer the reader to Ref. 24 for a complete discussion.

For the case of a small deformation $\mathbf{u}$ that is applied to the atoms of a crystal adiabatically through the perturbation parameter $\lambda(t)$, the CRG contribution to linear order in the velocity is

$$\dot{\lambda}\hat{H}^{(\dot{\lambda})} = -\frac{1}{2}\left(\hat{\mathbf{A}}\cdot\hat{\mathbf{p}} + \hat{\mathbf{p}}\cdot\hat{\mathbf{A}} \right). \tag{D1}$$

Here $\mathbf{A}$ is not the vector potential of electromagnetism, but one that emerges when transforming from the static reference frame to the CRG one. For a monochromatic perturbation, it becomes just $\mathbf{A} = \dot{\lambda}\mathbf{u} = \dot{\lambda}e^{i\mathbf{q}\cdot\mathbf{r}}$, so

$$\hat{H}^{(\dot{\lambda}_\beta)}(\mathbf{q}) = -e^{i\mathbf{q}\cdot\hat{\mathbf{r}}}\left(\hat{p}_\beta + \frac{q_\beta}{2} \right) \tag{D2}$$

which we recognize as the local current operator [cf. Eq. (A4) or (B8)]. Therefore, the first-order, cell-periodic wavefunctions with respect to this perturbation are

$$|\partial_{\dot{\lambda}_\beta} u_{n\mathbf{k},\mathbf{q}}^\beta\rangle = \sum_m^{\mathrm{unocc}} \frac{|u_{m\mathbf{k},\mathbf{q}}\rangle\langle u_{m\mathbf{k},\mathbf{q}}| \left(\hat{p}_\beta^{\mathbf{k}} + q_\beta/2 \right) |u_{n\mathbf{k}}\rangle}{\epsilon_{m\mathbf{k},\mathbf{q}} - \epsilon_{n\mathbf{k}}}, \tag{D3}$$

and the (cell averaged) induced polarization from the CRG part of the metric perturbation is

$$\overline{P}_{\alpha,\beta}^{\mathbf{q},\,\mathrm{CRG}} = \frac{4}{N_k}\sum_{n\mathbf{k}}\langle u_{n\mathbf{k}}|\hat{\mathcal{J}}_\alpha^{\mathbf{k},\mathbf{q}}|\partial_{\dot{\lambda}_\beta} u_{n\mathbf{k},\mathbf{q}}^\beta\rangle. \tag{D4}$$

The contribution to the FxE coefficient is determined by taking the second derivative of $\overline{P}_{\alpha,\beta}^{\mathbf{q},\mathrm{CRG}}$ with respect to q:

$$\overline{P}_{\alpha,\beta}^{(2,\omega\nu),\,\mathrm{CRG}} = \left. \frac{\partial^2 \overline{P}_{\alpha,\beta}^{\mathbf{q},\mathrm{CRG}}}{\partial q_\omega \partial q_\nu} \right|_{\mathbf{q}=0}. \tag{D5}$$

The CRG contribution is closely related to the diamagnetic susceptibility, $\chi_{\alpha\beta}$. In fact, in the case where only local potentials are present in the Hamiltonian [so that $\hat{\mathcal{J}}_\beta^{\mathbf{k},\mathbf{q}} = -(\hat{p}_\beta^{\mathbf{k}} + q_\beta/2)$ in Eq. (D4)], Eq. (D5) has the same form

as the expressions for the magnetic susceptibility derived in, e.g., Refs. 32 and 35 [*cf.* Eq. (11) and Eq. (9) in those works, respectively].

The magnetic susceptibility relates the magnetization, $\mathbf{M}$, to the external magnetic field, $\mathbf{B}$, via $M_\gamma = \chi_{\gamma\lambda}^{\text{mag}} B_\lambda$. This can be rewritten to relate the bound currents to the vector potential,

$$J_\alpha = \epsilon^{\alpha\zeta\gamma} \nabla_\zeta \chi_{\gamma\lambda} \epsilon^{\lambda\rho\beta} \nabla_\rho A_\beta, \tag{D6}$$

so that

$$\overline{P}_{\alpha,\beta}^{\mathbf{q},\,\text{CRG}} \sim \epsilon^{\alpha\zeta\gamma} q_\zeta \chi_{\gamma\lambda} \epsilon^{\beta\lambda\rho} q_\rho, \tag{D7}$$

where we have expressed the spatial derivatives in reciprocal space and canceled the resulting negative sign by permutating the second Levi-Civita symbol. Performing the $\mathbf{q}$-derivatives in Eq. (D5) gives

$$\overline{P}_{\alpha,\beta}^{(2,\omega\nu),\,\text{CRG}} = \sum_{\gamma\lambda} \left(\epsilon^{\alpha\omega\gamma} \epsilon^{\beta\lambda\nu} + \epsilon^{\alpha\nu\gamma} \epsilon^{\beta\lambda\omega} \right) \chi_{\gamma\lambda}. \tag{D8}$$

In the case that nonlocal potentials are present in the Hamiltonian, a calculation of the magnetic susceptibility would involve replacing the "displacement velocity" operator, $-\left(\hat{p}_\beta^{\mathbf{k}} + q_\beta/2\right)$, in Eq. (D3) with the full electromagnetic current operator from Eq. (53), as well as evaluating extra terms originating from the second-order Hamiltonian.[33,34,37] This is in contrast to the case of the CRG contribution we would like to calculate, where the only change in the case of nonlocal potentials is replacing $\hat{\mathcal{J}}_\alpha^{\mathbf{k},\mathbf{q}}$ in Eq. (D4) with the full current operator from Eq. (53); Eqs. (D2) and (D3) are unchanged. Therefore, Eq. (D4) does not strictly correspond to the magnetic susceptibility in this case. However, we show in Sec. VI that the numerical values are quite similar to previously calculated diamagnetic susceptibilities .

Appendix E: Divergence of the current at the atomic site for the PM path

To illustrate the point that nonlocal pseudopotentials allow unphysical transfer of charge between $\mathbf{r}$ and $\mathbf{r}'$, we shall consider the PM[34] definition of the current density, which provides a particularly transparent manifestation of such unphysical behavior. For simplicity, we focus our attention on a single atomic sphere [so we drop the ζ index of Eq. (48)], and we set the corresponding nuclear site as the coordinate origin. (There is no approximation here, as the contributions from different sites are spatially separated and additive.) Now suppose we wish to evaluate the nonlocal current density at the point $\mathbf{r}_0$. We need then to calculate Eq. (39) with Eq. (48), using a Dirac delta as a vector potential,

$$\mathbf{A}(\mathbf{r}) = A\hat{\mathbf{r}}_0 \, \delta(\mathbf{r} - \mathbf{r}_0) = A\hat{\mathbf{r}}_0 \delta(\hat{\mathbf{r}} - \hat{\mathbf{r}}_0) \frac{\delta(r - r_0)}{4\pi r^2}, \tag{E1}$$

where the caret above the position variable denotes a direction (not to be confused with the position operator), and in the second equality we have written the Dirac delta function in spherical coordinates. We choose the vector potential to be oriented along the radial direction, as this is the only allowed component within the PM theory: it is easy to see that a purely tangential $\mathbf{A}$ field yields a vanishing nonlocal contribution to the current [see Eq. (48)]. Then, the line integral needed for the first order term in Eq. (43) is

$$\begin{aligned}
\int_{\mathbf{s}' \to 0 \to \mathbf{s}} \mathbf{A} \cdot d\ell &= \int_0^1 \mathbf{A}(\tau\mathbf{s}) \cdot \mathbf{s} d\tau - \int_0^1 \mathbf{A}(\tau\mathbf{s}') \cdot \mathbf{s}' d\tau \\
&= A\hat{\mathbf{r}}_0 \cdot \left[\delta(\hat{\mathbf{s}} - \hat{\mathbf{r}}_0)\mathbf{s} \int_0^1 \frac{\delta(\tau s - r_0)}{4\pi(s\tau)^2} d\tau - \delta(\hat{\mathbf{s}}' - \hat{\mathbf{r}}_0)\mathbf{s}' \int_0^1 \frac{\delta(\tau s' - r_0)}{4\pi(s'\tau)^2} d\tau \right] \\
&= \frac{A}{4\pi r_0^2} \left[\delta(\hat{\mathbf{s}} - \hat{\mathbf{r}}_0)\theta(s - r_0) - \delta(\hat{\mathbf{s}}' - \hat{\mathbf{r}}_0)\theta(s' - r_0) \right],
\end{aligned} \tag{E2}$$

where θ is the Heaviside step function. Therefore, we can write the current-density operator as (recall that the tangential components vanish, so the current is purely radial)

$$\langle \mathbf{s} | \hat{\mathcal{J}}(\mathbf{r}) | \mathbf{s}' \rangle = \frac{i V^{\text{nl}}(\mathbf{s}, \mathbf{s}')}{4\pi r^2} \left[\delta(\hat{\mathbf{s}} - \hat{\mathbf{r}})\theta(s - r) - \delta(\hat{\mathbf{s}}' - \hat{\mathbf{r}})\theta(s' - r) \right]. \tag{E3}$$

Considering a general time-dependent wavefunction as in Eq. (8), the current density is

$$\mathbf{J}^{\mathrm{nl}}(\mathbf{r}, t) = \frac{i\hat{\mathbf{r}}}{4\pi r^2} \int d^3 s \int d^3 s' \Psi^*(\mathbf{s}, t)\Psi(\mathbf{s}', t) V^{\mathrm{nl}}(\mathbf{s}, \mathbf{s}') \left[\delta(\hat{\mathbf{s}} - \hat{\mathbf{r}})\theta(s - r) - \delta(\hat{\mathbf{s}}' - \hat{\mathbf{r}})\theta(s' - r)\right]$$

$$= \frac{i\hat{\mathbf{r}}}{r^2} \sum_{lm} \int_r^\infty ds \left[\langle\phi_{lm}|\Psi(t)\rangle\Psi^*(s\hat{\mathbf{r}}, t)\phi_{lm}(s\hat{\mathbf{r}}) - \langle\Psi(t)|\phi_{lm}\rangle\Psi(s\hat{\mathbf{r}}, t)\phi_{lm}^*(s\hat{\mathbf{r}})\right] s^2 \qquad \text{(E4)}$$

$$= \frac{\hat{\mathbf{r}}}{r^2} \int_r^\infty ds\, \rho^{\mathrm{nl}}(s\hat{\mathbf{r}})s^2$$

where we have identified the nonlocal charge $\rho^{\mathrm{nl}}(\mathbf{r}) = -i\langle\Psi| \left[|\mathbf{r}\rangle\langle\mathbf{r}|, \hat{V}^{\mathrm{nl}}\right] |\Psi\rangle$ [*cf.* Eq. (32)]. Note that the upper limit of the integral can be set to r_{c}, i.e., the core radius that was used in the generation of the pseudopotential (the nonlocal current density field is strictly contained within a sphere of radius r_{c}). This shows that, in the special case of the Pickard-Mauri theory, the nonlocal density does, in fact, provide complete information about the current density.

Unfortunately, a consequence of the above derivations is that the nonlocal current density *diverges* as $|\mathbf{r} - \mathbf{R}|^{-2}$ in the vicinity of an atomic site $\mathbf{R}$. To see this it suffices to observe that the integral in the above equation tends, for $r \to 0$, to a direction-dependent constant,

$$\int_0^{+\infty} s^2 ds\, \rho^{\mathrm{nl}}(s\hat{\mathbf{r}}) = C(\hat{\mathbf{r}}). \qquad \text{(E5)}$$

Thus, the current-density field diverges near the atomic site as

$$\mathbf{J}^{\mathrm{nl}}(\mathbf{r}) \sim \frac{\hat{\mathbf{r}}C(\hat{\mathbf{r}})}{r^2}. \qquad \text{(E6)}$$

[1] M. S. Majdoub, R. Maranganti, and P. Sharma, Phys. Rev. B **79**, 115412 (2009).

[2] D. Lee, A. Yoon, S. Y. Jang, J.-G. Yoon, J.-S. Chung, M. Kim, J. F. Scott, and T. W. Noh, Phys. Rev. Lett. **107**, 057602 (2011).

[3] P. V. Yudin, A. K. Tagantsev, E. A. Eliseev, A. N. Morozovska, and N. Setter, Phys. Rev. B **86**, 134102 (2012).

[4] A. Y. Borisevich, E. Eliseev, A. Morozovska, C.-J. Cheng, J.-Y. Lin, Y.-H. Chu, D. Kan, I. Takeuchi, V. Nagarajan, and S. V. Kalinin, Nat. Commun. **3**, 775 (2012).

[5] G. Catalan, L. Sinnamon, and J. Gregg, J. Phys.: Conden. Mat. **16**, 2253 (2004).

[6] G. Catalan, B. Noheda, J. McAneney, L. J. Sinnamon, and J. M. Gregg, Phys. Rev. B **72**, 020102 (2005).

[7] H. Zhou, J. Hong, Y. Zhang, F. Li, Y. Pei, and D. Fang, Physica B: Condensed Matter **407**, 3377 (2012).

[8] A. N. Morozovska, E. A. Eliseev, M. D. Glinchuk, L.-Q. Chen, and V. Gopalan, Phys. Rev. B **85**, 094107 (2012).

[9] W. Zhu, J. Y. Fu, N. Li, and L. Cross, Applied Physics Letters **89**, 192904 (2006).

[10] U. K. Bhaskar, N. Banerjee, A. Abdollahi, Z. Wang, D. G. Schlom, G. Rijnders, and G. Catalan, Nat. Nanotechnol. **11**, 263 (2016).

[11] H. Lu, C.-W. Bark, D. Esque de los Ojos, J. Alcala, C. B. Eom, G. Catalan, and A. Gruverman, Science **336**, 59 (2012).

[12] A. Gruverman, B. J. Rodriguez, A. Kingon, R. Nemanich, A. Tagantsev, J. Cross, and M. Tsukada, Applied Physics Letters **83**, 728 (2003).

[13] P. Zubko, G. Catalan, and A. K. Tagantsev, Annual Review of Materials Research **43**, 387 (2013).

[14] P. V. Yudin and A. K. Tagantsev, Nanotechnology **24**, 432001 (2013).

[15] M. Stengel, Phys. Rev. B **88**, 174106 (2013).

[16] J. Hong and D. Vanderbilt, Phys. Rev. B **84**, 180101 (2011).

[17] J. Hong and D. Vanderbilt, Phys. Rev. B **88**, 174107 (2013).

[18] The FxE response of any finite crystal also has an important contribution from the surface, as discussed in Refs. 21 and 56, and calculated using density-functional theory for $SrTiO_3$ in 19. In this work, we will exclusively focus on bulk contribution, which poses a more significant challenge for a computational treatment.

[19] M. Stengel, Phys. Rev. B **90**, 201112 (2014).

[20] S. Baroni, S. de Gironcoli, A. Dal Corso, and P. Giannozzi, Rev. Mod. Phys. **73**, 515 (2001).

[21] M. Stengel, Nat. Commun. **4**, 2693 (2013).

[22] R. D. King-Smith and D. Vanderbilt, Phys. Rev. B **47**, 1651 (1993).

[23] R. Resta, Rev. Mod. Phys. **66**, 899 (1994).

[24] M. Stengel and D. Vanderbilt, (2018), arXiv:1806.05587 [cond-mat.mtrl-sci].

[25] J. Sakuri and J. Napolitano, *Modern Quantum Mechanics–2nd ed.* (Addison-Wesley, San Fransisco, CA, 1994).

[26] C. Li, L. Wan, Y. Wei, and J. Wang, Nanotechnology **19**, 155401 (2008).

[27] D. Vanderbilt, Phys. Rev. B **41**, 7892 (1990).

[28] D. R. Hamann, M. Schlüter, and C. Chiang, Phys. Rev. Lett. **43**, 1494 (1979).

[29] L. Kleinman and D. M. Bylander, Phys. Rev. Lett. **48**, 1425 (1982).

[30] P. E. Blöchl, Phys. Rev. B **50**, 17953 (1994).

[31] P. Umari, A. D. Corso, and R. Resta, AIP Conference Proceedings **582**, 107 (2001).

[32] G. Vignale, Phys. Rev. Lett. **67**, 358 (1991).

[33] S. Ismail-Beigi, E. K. Chang, and S. G. Louie, Phys. Rev. Lett. **87**, 087402 (2001).

[34] C. J. Pickard and F. Mauri, Phys. Rev. Lett. **91**, 196401 (2003).

[35] F. Mauri and S. G. Louie, Phys. Rev. Lett. **76**, 4246 (1996).

[36] F. Mauri, B. G. Pfrommer, and S. G. Louie, Phys. Rev. Lett. **77**, 5300 (1996).

[37] C. J. Pickard and F. Mauri, Phys. Rev. B **63**, 245101 (2001).

[38] C. J. Pickard and F. Mauri, Phys. Rev. Lett. **88**, 086403 (2002).

[39] J. Nye, *Physical Properties of Crystals: Their Representation by Tensors and Matrices*, Oxford science publications (Clarendon Press, 1985).

[40] A. Messiah, *Quantum Mechanics, Vol. 2* (North-Holland, 1981) p. 752.

[41] D. J. Thouless, Phys. Rev. B **27**, 6083 (1983).

[42] Q. Niu and D. J. Thouless, J. Phys. A: Math. and Gen. **17**, 2453 (1984).

[43] M. V. Berry, P. Roy Soc. Lond. A Mat. **392**, 45 (1984).

[44] X. Gonze, Phys. Rev. B **55**, 10337 (1997).

[45] S. L. Adler, Phys. Rev. **126**, 413 (1962).

[46] Note that the definition of Eq. (22) involves a choice of convention in that the exponential factor $e^{i\mathbf{q}\cdot\mathbf{r}}$ is placed to the right of $\hat{\mathcal{J}}_\alpha(\mathbf{q})$ as opposed to the left. Choosing the opposite convention would simply switch the operators between the two terms in Eq. (23).

[47] A. F. Starace, Phys. Rev. A **3**, 1242 (1971).

[48] M. S. Hybertsen and S. G. Louie, Phys. Rev. B **35**, 5585 (1987).

[49] P. Giannozzi, S. de Gironcoli, P. Pavone, and S. Baroni, Phys. Rev. B **43**, 7231 (1991).

[50] A. Dal Corso, S. Baroni, and R. Resta, Phys. Rev. B **49**, 5323 (1994).

[51] A. M. Essin, A. M. Turner, J. E. Moore, and D. Vanderbilt, Phys. Rev. B **81**, 205104 (2010).

[52] In contrast to the ICL straight-line path, Eq. (42) using the PM $\mathbf{s}' \to \mathbf{R}_\zeta \to \mathbf{s}$ path [i.e., the phase in Eq. (48) multiplying the entire Hamiltonian instead of just $V^{\mathrm{nl}}(\mathbf{s}, \mathbf{s}')$] does *not* recover $\hat{\mathcal{J}}_\alpha^{\mathrm{loc}}$ for local potentials.

[53] R. M. Martin, Phys. Rev. B **5**, 1607 (1972).

[54] D. Vanderbilt, J. Phys. Chem. Sol. **61**, 147 (2000).

[55] Recall that in Ref. 24, this contribution is referred to as the "dynamic" gauge-field term.

[56] M. Stengel and D. Vanderbilt, in *Flexoelectricity in Solids From Theory to Applications*, edited by A. K. Tagantsev and P. V. Yudin (World Scientific Publishing Co., Singapore, 2016) Chap. 2, pp. 31–110.

[57] X. Gonze, B. Amadon, P.-M. Anglade, J.-M. Beuken, F. Bottin, P. Boulanger, F. Bruneval, D. Caliste, R. Caracas, M. Ct, T. Deutsch, L. Genovese, P. Ghosez, M. Giantomassi, S. Goedecker, D. Hamann, P. Hermet, F. Jollet, G. Jomard, S. Leroux, M. Mancini, S. Mazevet, M. Oliveira, G. Onida, Y. Pouillon, T. Rangel, G.-M. Rignanese, D. Sangalli, R. Shaltaf, M. Torrent, M. Verstraete, G. Zerah, and J. Zwanziger, Computer Physics Communications **180**, 2582 (2009).

[58] J. P. Perdew, K. Burke, and M. Ernzerhof, Phys. Rev. Lett. **77**, 3865 (1996).

[59] X. Gonze, Phys. Rev. B **55**, 10337 (1997).

[60] X. Gonze and C. Lee, Phys. Rev. B **55**, 10355 (1997).

[61] D. R. Hamann, Phys. Rev. B **88**, 085117 (2013).

[62] H. J. Monkhorst and J. D. Pack, Phys. Rev. B **13**, 5188 (1976).

[63] R. M. Pick, M. H. Cohen, and R. M. Martin, Phys. Rev. B **1**, 910 (1970).

[64] H. P. R. Frederikse and G. A. Candela, Phys. Rev. **147**, 583 (1966).

[65] This can be deduced from Eq.(12) and (13) of Ref. 34: By placing a single spherical pseudoatom in the gauge origin, all nonlocal contributions vanish by construction as they are multiplied by $\mathbf{R}$; thus, the applied magnetic field enters the Hamiltonian via the usual substitution $\mathbf{p} \to \mathbf{p}+\mathbf{A}$. Then, the first order Hamiltonian is the angular momentum operator, which commutes with the ground-state density matrix and yields a vanishing linear response, and the second-order piece picks the quadrupolar moment of the ground-state density, as in the local case.

[66] F. S. Khan and P. B. Allen, Phys. Rev. B **29**, 3341 (1984).

[67] R. M. Martin, *Electronic structure: basic theory and practical methods* (Cambridge university press, 2004).